

# CO<sub>2</sub> corrosion of mild steel

7

Aria Kahyarian<sup>1</sup>, Mohsen Achour<sup>2</sup> and Srdjan Nesic<sup>1</sup>

<sup>1</sup>Ohio University, Athens, OH, United States; <sup>2</sup>ConocoPhillips, Bartlesville, OK, United States

## 7.1 Introduction

Produced oil and gas are always accompanied by some water and varying amounts of carbon dioxide and in some cases hydrogen sulfide and organic acids. All of these may affect the integrity of mild steel. This has been known for over 100 years, yet internal corrosion of pipelines and other facilities made from mild steel still represents a challenge for the oil and gas industry. Although many corrosion-resistant alloys are able to withstand this type of corrosion, it is a matter of economics: mild steel is still the most cost-effective construction material. The price of failure due to internal corrosion is enormous, both in terms of direct costs, such as repair/replacement costs and lost production, and indirect costs, such as environmental cost and impact on the downstream industries.

The following text summarizes the current degree of understanding of CO<sub>2</sub> corrosion of mild steel exposed to aqueous environments. Much has been understood about the basic mechanisms, enabling construction of mechanistic prediction models, but many challenges remain, particularly when it comes to effects of corrosion product layers, multiphase flow, additional species, hydrocarbon composition, inhibition, etc. The following sections start out with describing the basic physicochemical phenomena underlying CO<sub>2</sub> corrosion and gradually move to more complicated situations, culminating with the list of multifaceted real-life challenges seen in the field.

## 7.2 Water chemistry in CO<sub>2</sub> corrosion

Carbon dioxide (CO<sub>2</sub>) is a stable, inert, and noncorrosive gas. However, upon dissolution in water and a subsequent hydration reaction, a more reactive chemical species, carbonic acid (H<sub>2</sub>CO<sub>3</sub>), is formed. This reaction is followed by dissociation reactions to form bicarbonate (HCO<sub>3</sub><sup>-</sup>) ion, carbonate (CO<sub>3</sub><sup>2-</sup>) ion, and hydrogen (H<sup>+</sup>) ion, resulting in an acidic and corrosive solution. The reactions associated with these chemical equilibria and their corresponding mathematical relationship are listed in Table 7.1.

The chemical equilibria and water chemistry associated with dissolved CO<sub>2</sub> and its carbonate derivatives have been extensively studied [1–9]. The first step, CO<sub>2</sub> dissolution, is described via Eq. (7.1), where K<sub>CO<sub>2</sub></sub> is the proportionality constant and can be expressed as Henry's constant for the simplest case of ideal gas and ideal solution. The nonideal behavior of the gas phase, represented by fugacity coefficient, and the liquid

**Table 7.1 Chemical reactions of acidic water/CO<sub>2</sub> equilibria**

Reaction	Equilibrium equation	
$\text{CO}_{2(\text{g})} \rightleftharpoons \text{CO}_{2(\text{aq})}$	$K_{\text{CO}_2} = \frac{[\text{CO}_{2(\text{aq})}]}{p\text{CO}_{2(\text{g})}}$	(7.i)
$\text{CO}_{2(\text{aq})} + \text{H}_2\text{O}_{(\text{l})} \rightleftharpoons \text{H}_2\text{CO}_{3(\text{aq})}$	$K_{\text{hyd}} = \frac{[\text{H}_2\text{CO}_3]}{[\text{CO}_{2(\text{aq})}]}$	(7.ii)
$\text{H}_2\text{CO}_{3(\text{aq})} \rightleftharpoons \text{HCO}_3^-(\text{aq}) + \text{H}^+(\text{aq})$	$K_{\text{ca}} = \frac{[\text{HCO}_3^-][\text{H}^+]}{[\text{H}_2\text{CO}_3]}$	(7.iii)
$\text{HCO}_3^-(\text{aq}) \rightleftharpoons \text{CO}_3^{2-}(\text{aq}) + \text{H}^+(\text{aq})$	$K_{\text{bi}} = \frac{[\text{CO}_3^{2-}][\text{H}^+]}{[\text{HCO}_3^-]}$	(7.iv)
$\text{H}_2\text{O}_{(\text{l})} \rightleftharpoons \text{OH}^-(\text{aq}) + \text{H}^+(\text{aq})$	$K_w = [\text{OH}^-][\text{H}^+]$	(7.v)

phase, represented by activity coefficients, can be incorporated into the proportionality constant following the extended Rault's law.

The product of CO<sub>2</sub> hydration (reaction 7.ii), carbonic acid (H<sub>2</sub>CO<sub>3</sub>), is a diprotic weak acid. The term *weak acid* refers to the fact that this species is only partially dissociated in an aqueous solution. With the first dissociation constant of pK<sub>ca</sub> ≈ 3.6 (reaction 7.iii) and the second dissociation constant of pK<sub>bi</sub> ≈ 10.33 (reaction 7.iv), the carbonic acid dissociation reaction can be considered as the main source of acidity (H<sup>+</sup>) in the solution. Although water can also be categorized as a weak acid, with pK<sub>a</sub> ≈ 14, it has no significant effect when compared with H<sub>2</sub>CO<sub>3</sub> and HCO<sub>3</sub><sup>-</sup>.

The chemical equilibria shown in Table 7.1 represent a simple case of CO<sub>2</sub> dissolution in pure water, such as what is observed in condensed water formed in wet gas pipelines. However, a more complex water chemistry is found in formation water, where significant amounts of various ions such as Cl<sup>-</sup>, Na<sup>+</sup>, Ca<sup>+</sup>, SO<sub>4</sub><sup>2-</sup>, organic acid (such as acetic acid, formic acid, and propionic acid), as well as hydrogen sulfide can be present [10,11]. These species can significantly alter the speciation of CO<sub>2</sub> equilibria by changing the acidity and ionic strength of the solution.

A more comprehensive discussion on the chemical speciation of CO<sub>2</sub>/water system is provided in Chapter 34.

### 7.3 Electrochemistry of CO<sub>2</sub> corrosion

The aqueous CO<sub>2</sub> corrosion of mild steel, as seen in oil and gas industry, is by nature an electrochemical system. The spontaneous iron dissolution, causing the deterioration of the metallic structure, is an electrochemical oxidation process. On the other hand, the cathodic hydrogen evolution reaction provides the required electron sink for the iron dissolution to progress. In the CO<sub>2</sub> corrosion context, the hydrogen evolution reaction is a family of cathodic reactions with all having molecular hydrogen as their

**Table 7.2 Electrochemical reactions associated with aqueous acidic CO<sub>2</sub> corrosion of mild steel**

Electrochemical reaction	Dominant reaction type	
$H_{(aq)}^+ + e^- \rightleftharpoons \frac{1}{2}H_{2(g)}$	Cathodic	(7.vi)
$H_2O_{(l)} + e^- \rightleftharpoons OH_{(aq)}^- + \frac{1}{2}H_{2(g)}$	Cathodic	(7.vii)
$H_2CO_{3(aq)} + e^- \rightleftharpoons HCO_{3(aq)}^- + \frac{1}{2}H_{2(g)}$	Cathodic	(7.viii)
$HCO_{3(aq)}^- + e^- \rightleftharpoons CO_{3(aq)}^{2-} + \frac{1}{2}H_{2(g)}$	Cathodic	(7.ix)
$Fe_{(aq)}^{2+} + 2e^- \rightleftharpoons Fe_{(s)}$	Anodic	(7.x)

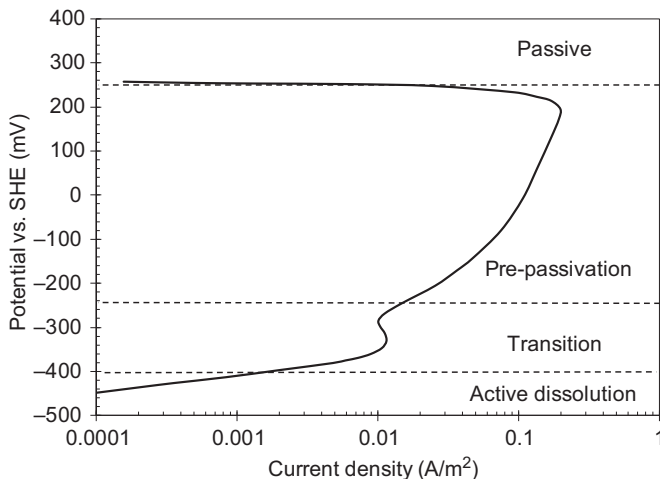
product. That includes the reduction of H<sup>+</sup>, H<sub>2</sub>CO<sub>3</sub>, HCO<sub>3</sub><sup>-</sup>, and H<sub>2</sub>O, as shown in Table 7.2. Considering the chemical equilibrium of the water/CO<sub>2</sub> system, it can be shown that all these reactions are thermodynamically identical. This means that they have the same reversible potential (based on Nernst equation), if the concentrations of the involved chemical species are defined by the equilibrium speciation. Hence, the main difference resides in reaction kinetics. The same would also hold true for other weak acids, such as acetic acid and hydrogen sulfide.

Table 7.2 summarizes the commonly accepted electrochemical reactions associated with aqueous CO<sub>2</sub> corrosion of mild steel. Reactions (7.vi)–(7.ix) are the hydrogen evolution reactions in a water/CO<sub>2</sub> solution. Reactions (7.vi) and (7.vii) are the hydrogen ion and water reduction reactions, respectively. Reaction (7.viii) is the reduction of carbonic acid (H<sub>2</sub>CO<sub>3</sub>), and reaction (7.ix) is the reduction of bicarbonate ion, which is believed to be significant at near-neutral and alkaline pH values because of the high bicarbonate ion concentration [12–15].

### 7.3.1 Anodic reactions

The iron oxidation as the dominant anodic reaction is a key element in acidic corrosion of mild steel. The mechanism of iron oxidation reaction in acidic media has been the subject of numerous studies over the last half a century [16–27] and has been proved difficult to explain. In this section, the mechanism of acidic iron dissolution is briefly discussed to provide the necessary context relevant to CO<sub>2</sub> corrosion; a thorough review of the existing literature can be found elsewhere [26,28].

El Miligy et al. [19] showed that the iron dissolution in mildly acidic environments occurs in four different states, depending on the electrode potential. The authors categorized these as *active dissolution*, *transition*, *prepassivation*, and *passive*, as demonstrated in Fig. 7.1. Each range was shown to have a different electrochemical behavior, characterized by different apparent Tafel slopes and reaction orders. The two local current maxima, observed in transition and prepassivation ranges, were showed to be also pH dependent. This suggests that the mechanism of iron dissolution at corrosion potential could depend on the solution pH and other environmental conditions.



**Figure 7.1** Anodic polarization curve of iron in 0.5 M Na<sub>2</sub>SO<sub>4</sub> solution at pH 5 and 298K, with the scan rate of 6.6 mV/s and rotating disk electrode at 69 rps. *SHE*, standard hydrogen electrode.

Adapted from A.A. El Miligy, D. Geana, W.J. Lorenz, A theoretical treatment of the kinetics of iron dissolution and passivation, *Electrochimica Acta* 20 (1975) 273–281.

For the case of CO<sub>2</sub> corrosion, at pH values less than 5, the experimental results suggest that the corrosion is occurring at the active dissolution range [29,30]. At pH values more than 5, the corrosion potential gradually shifts towards the transition range, and eventually reaches the prepassivation range at near neutral pH values [20].

The complex behavior depicted in Fig. 7.1 is an indication of a reaction mechanism with multiple intermediate species and rate-determining steps. In the literature, there are two main mechanisms proposed for iron dissolution in acidic solutions: the “catalytic mechanism” and the “consecutive mechanism.” These two mechanisms are associated with two distinct electrochemical behaviors observed specifically in the active dissolution range. The catalytic mechanism, first proposed by Heusler et al. [31], is based on the experimental Tafel slope of 30 mV and second-order dependence on hydroxide (OH<sup>-</sup>) ion concentration. On the other hand, the consecutive mechanism proposed by Bockris et al. [24] was formulated to explain the observed Tafel slope of 40 mV and a first-order dependence on (OH<sup>-</sup>) ion concentration. These two significantly different reaction kinetics are believed to be caused by the surface activity of the iron electrode [17], i.e., the dissolution of cold-worked iron electrodes with high internal stress occurs with a 30 mV Tafel slope, whereas a 40 mV Tafel slope was observed for dissolution of recrystallized iron [17,25,27,28]. The catalytic mechanism is described as reactions (7.xi)–(7.xiv) [28].





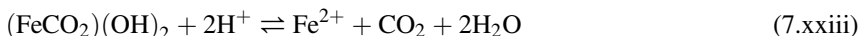
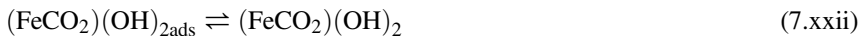
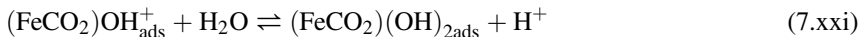
This mechanism suggests that the  $(\text{FeOH})_{\text{ads}}$  on the so-called kink sites acts as a catalyst in the iron dissolution reaction. Although this mechanism has been criticized because of the two-electron transfer step (reaction 7.xiii) [25], it has been supported by atomistic scale discussions and electrochemical impedance measurements [21,22,27].

The consecutive mechanism [24] shares the same initial and final step with the “catalytic mechanism,” as shown in reactions (7.xv)–(7.xvii). However, in this mechanism,  $(\text{FeOH})_{\text{ads}}$  is directly oxidized through a one-electron transfer elementary step (reaction 7.xvi).



The anodic polarization curves obtained for mild steel dissolution in CO<sub>2</sub>-saturated environments have frequently been reported to have a 40 mV Tafel slope and a first-order dependence on hydroxide ion concentration [13,15,29,30,32], in accordance with the “consecutive mechanism” proposed by Bockris et al. [24]. Hence, this mechanism and its corresponding kinetic relationship have been commonly used to describe the anodic currents in CO<sub>2</sub> corrosion of mild steel [29,30,33–36]. On the other hand, although a few studies report a rather significant effect of CO<sub>2</sub> and other carbonate species on the acidic iron dissolution reaction [13,20], in-depth analysis on the extent of these possible effects is rarely available in the literature. In a study by Nešić et al. [20], the anodic polarization curves were used to discuss the effect of CO<sub>2</sub> in a short potential range (~100 mV) above the corrosion potential. The experiments were performed in perchlorate solutions, in the pH range of 2–6 and pCO<sub>2</sub> from 0 to 1 bar. In that study, the authors reported the Tafel slope of 30 mV and second-order dependence on OH<sup>−</sup> ion concentration for pH values less than 4 (corresponding to the “catalytic mechanism”). In the pH range of 4–6, the reported Tafel slopes were gradually increasing, whereas the dependence on OH<sup>−</sup> ion concentration was diminishing. Ultimately, at pH ~ 6, a Tafel slope of 120 mV with zero dependence on OH<sup>−</sup> ion concentration was reported. The results showed that the presence of CO<sub>2</sub> does not affect the observed Tafel slopes, whereas the exchange current densities were linearly proportional to pCO<sub>2</sub> over the studied pH range. The authors formulated the following mechanism to describe the effect of CO<sub>2</sub> on iron dissolution.





Although this complex mechanism was not supported with sufficient experimental evidence, the proposed steps resemble the so-called branching mechanism proposed by Drazic et al. [25]. Here the authors suggest a direct  $\text{CO}_2$  adsorption onto the iron surface forming the surface species  $(\text{FeCO}_2)_{\text{ads}}$ , which acts as an active site for OH adsorption.

### 7.3.2 Cathodic reactions

The mechanism of hydrogen evolution reaction from  $\text{H}^+$  ions on various metals has been extensively studied [37–44]. This reaction is commonly believed to consist of three elementary steps as shown in reactions (7.xxiv)–(7.xxvi) [45]. Reaction (7.xxiv), commonly referred to as the Volmer step, is the electrochemical adsorption and reduction of  $\text{H}^+$  ions from the solution. This reaction is succeeded by a desorption step, either the electrochemical desorption reaction (7.xxv) (Heyrovsky step) or the chemical desorption reaction (Tafel step). Other alternative elementary steps such as the so-called surface diffusion step or the ones involving molecular hydrogen ion ( $\text{H}_2^+$ ) have also been proposed in the literature [46,47]. The kinetic parameters of the overall reaction, apparent Tafel slope and reaction order, are defined by the rate-determining step and have been shown to be influenced by numerous parameters such as the electrode material [38,48–50], surface crystal structure [50,51], pH [52,53], overpotential [49,53], adsorbed species, and trace impurities [43,50,54,55]. This suggests a significant variation of the reaction mechanism, and therefore, the apparent kinetic parameters, with rather slight changes in the surface properties and/or the environmental conditions.



The  $\text{H}^+$  reduction reaction on an iron surface is commonly assumed to be limited by the rate of the Volmer step (reaction 7.xxvii) [20,56–60], as suggested in the studies by Bockris and coworkers [38,42,43,61]. This rate-determining step is associated with

a theoretical Tafel slope of  $2 \times 2.303RT/F$  and the reaction order of 1 versus  $H^+$  concentration [62]. Although these theoretical values have been confirmed in a number of studies [63–65], some deviations are also reported in the literature [23,66]. On the other hand, the verification of this mechanism at mildly acidic and near-neutral environments, which are more relevant to the CO<sub>2</sub> corrosion conditions, is lacking because of the interference from the iron dissolution reaction.

The mechanism of hydrogen evolution from weak acids has been described based on an analogy with that of the hydrogen ion reduction. Using a generic formulation, the elementary steps are shown in reactions (7.xxvii)–(7.xxix), where HA denotes any weak acid, such as H<sub>2</sub>CO<sub>3</sub>, HCO<sub>3</sub><sup>−</sup>, H<sub>2</sub>O, and H<sub>2</sub>S, or any of the weak carboxylic acids, such as acetic acid [14,57,67–69].



For hydrogen evolution from water, assuming the Volmer step (reaction 7.xxvii) to be rate determining, a theoretical Tafel slope of  $2 \times 2.303RT/F$  is expected with no pH dependence of the reaction rate. It has frequently been demonstrated that the solution pH does not affect the rate of water reduction in the acidic and near-neutral pH range; however, the reported Tafel slopes are significantly deviating from the theoretically expected value of  $2 \times 2.303RT/F$  [15,16,30,64,66].

The mechanistic details of the hydrogen evolution reaction from other weak acids such as H<sub>2</sub>CO<sub>3</sub> and HCO<sub>3</sub><sup>−</sup> are rarely discussed in the literature. In the few studies addressing this subject [13,70], the proposed mechanisms are based on the same elementary steps as discussed above. However, systematic investigations on this subject are still lacking, probably because of the experimentation challenges resulting from the interference by  $H^+$  and H<sub>2</sub>O reduction reactions. On the other hand, considering the exchange current density expressions, commonly used in the literature for describing the rate of these reactions [12,71,72], it is generally assumed that the rate of all hydrogen-evolving reactions involved in CO<sub>2</sub> corrosion is limited by the Volmer step (reaction 7.xxvii).

### 7.3.3 Charge transfer rate calculations

The charge transfer rates are often expressed in terms of the Tafel or the Butler–Volmer relationships, using two main parameters, exchange current density and overpotential. The application of these relationships to CO<sub>2</sub> corrosion and the theoretical derivation of their associated parameters were discussed in more detail elsewhere [73]. Both the Tafel and the Butler–Volmer are well-known fundamental equations used to model the kinetics of reversible electrochemical reaction. However, in CO<sub>2</sub> corrosion, the reversibility of the electrochemical reactions is not the focus. Here, the dominating anodic reaction is iron dissolution, and the hydrogen-evolving

reactions are the dominant cathodic reactions. The reverse reactions, iron deposition and hydrogen oxidation, are commonly assumed to be negligible, for the typical conditions in CO<sub>2</sub> corrosion.

The application of the Butler–Volmer relationship to describe the rate of electrochemical reaction relevant to CO<sub>2</sub> corrosion results in overly complicated mathematical expressions and, in some cases, inconsistencies at a basic level. For example, the reversible potential of the hydrogen evolution reactions is a function of  $p\text{H}_2$ , as described by the Nernst equation. In the literature, it is commonly assumed that  $p\text{H}_2 = 1$  bar [29,71,74], which is never the case in typical laboratory or field conditions for the case of CO<sub>2</sub> corrosion. Invariably, dissolved H<sub>2</sub> is present only in minute and often indiscernible concentrations, as a product of cathodic reactions. To properly define a reversible potential, one needs to assume a constant, arbitrary value for  $p\text{H}_2$ . Such unnecessary complications can be avoided by simply expressing the rates, only based on the dominant half reactions. For example, the rate of cathodic half of generic reaction (7.xxx) can be expressed as Eq. (7.1).



$$i = nFk_0(C_{\text{O}}^s)^p e^{\left(\frac{-nF(E_{\text{app}}-E_0)}{RT}\right)} \quad (7.1)$$

where,  $k_0$  is the apparent reaction rate constant,  $C_{\text{O}}^s$  is the concentration of the reactant at the metal surface,  $p$  is the apparent reaction order,  $E_0$  is the standard potential,  $E_{\text{app}}$  is the applied potential, and other parameters have their common electrochemical meaning. Using this approach, simple current potential relationships for the electrochemical reactions associated with CO<sub>2</sub> corrosion can be formulated, as summarized in Table 7.3.

The values of the reaction rate constants for the reactions listed in Table 7.3 can be recalculated from the existing literature. Considering the Tafel equation (Eq. 7.2) along with Eq. (7.1), the relationship between exchange current density and reaction rate constant is shown in Eq. (7.3).

$$i = i_0 10^{\left(\frac{E_{\text{app}}-E_{\text{rev}}}{-b}\right)} \quad (7.2)$$

$$k_0 = \frac{i_0 10^{\left(\frac{-E_{\text{rev}}}{-b}\right)}}{nF(C_{\text{O,ref}}^b)^p e^{\left(\frac{-nF(-E_0)}{RT_{\text{ref}}}\right)}} \quad (7.3)$$

The reaction rate constant and other relevant electrochemical parameters required for charge transfer rate calculations are listed in Table 7.4.

**Table 7.3 Current potential relationships for the reactions listed in Table 7.2**

Electrochemical reaction	Mathematical relationship for half reaction <sup>a</sup>
Reaction (7.vi)	$i_{c,H^+} = -n_{H^+} F k_{OH^+} C_{H^+}^S e^{\left(\frac{-\alpha_{H^+} n_{H^+} F (E_{app} - E_{0H^+})}{RT}\right)}$
Reaction (7.vii)	$i_{c,H_2O} = -n_{H_2O} F k_{H_2O} e^{\left(\frac{-\alpha_{H_2O} n_{H_2O} F (E_{app} - E_{0H_2O})}{RT}\right)}$
Reaction (7.viii)	$i_{c,H_2CO_3} = -n_{H_2CO_3} F k_{H_2CO_3} C_{H_2CO_3}^S e^{\left(\frac{-\alpha_{H_2CO_3} n_{H_2CO_3} F (E_{app} - E_{0H_2CO_3})}{RT}\right)}$
Reaction (7.ix)	$i_{c,HCO_3^-} = -n_{HCO_3^-} F k_{HCO_3^-} C_{HCO_3^-}^S e^{\left(\frac{-\alpha_{HCO_3^-} n_{HCO_3^-} F (E_{app} - E_{0HCO_3^-})}{RT}\right)}$
Reaction (7.x)	$i_{a,Fe} = n_{Fe} F k_{0Fe} C_{OH^-}^S e^{\left(\frac{(2-\alpha_{Fe}) F (E_{app} - E_{0Fe})}{RT}\right)}$

<sup>a</sup> $i_c$  and  $i_a$  denote the current density calculations for cathodic half reactions and anodic half reactions, respectively.

**Table 7.4 Electrochemical parameters for the relationships in Table 7.3,**

$$\left(-\frac{\Delta H_j}{R} \left(\frac{1}{T} - \frac{1}{T_{j,ref}}\right)\right)$$

where  $k_{0j} = k_{0j,ref} e$

	$n_j$	$\alpha_j$	$E_{0,j}$ vs. SHE (V)	$k_{0j,ref}$	$\Delta H_j$ (kJ/mol)	$T_{j,ref}$ (K)
$j = Fe$	2	0.5 <sup>a</sup>	-0.447 <sup>b</sup>	$1.59 \times 10^5 \left(\frac{\text{mol}}{\text{s} \cdot \text{m}^2 \cdot \text{M}}\right)^a$	37.5 <sup>a</sup>	298.15 <sup>a</sup>
$j = H^+$	1	0.5 <sup>a</sup>	0.000	$5.18 \times 10^{-5} \left(\frac{\text{mol}}{\text{s} \cdot \text{m}^2 \cdot \text{M}}\right)^a$	30 <sup>a</sup>	298.15 <sup>a</sup>
$j = H_2O$	1	0.5 <sup>c</sup>	-0.8277 <sup>b</sup>	$2.70 \times 10^{-5} \left(\frac{\text{mol}}{\text{s} \cdot \text{m}^2}\right)^c$	30 <sup>c</sup>	293.15 <sup>c</sup>
$j = H_2CO_3$	1	0.5 <sup>a</sup>	-0.381 <sup>f</sup>	$3.71 \times 10^{-2} \left(\frac{\text{mol}}{\text{s} \cdot \text{m}^2 \cdot \text{M}}\right)^a$	50 <sup>a</sup>	293.15 <sup>a</sup>
$j = HCO_3^-$	1	0.5 <sup>d</sup>	-0.615 <sup>f</sup>	$7.37 \times 10^{-5} \left(\frac{\text{mol}}{\text{s} \cdot \text{m}^2 \cdot \text{M}}\right)^d$	50 <sup>e</sup>	298.15 <sup>e</sup>

Parameters obtained or recalculated from a, Nordsveen et al. [71]; b, CRC Handbook [75]; c, Zheng et al. [56]; d, Gray et al. [15]; e, Han et al. [12]; f, Linter and Burstein [76].

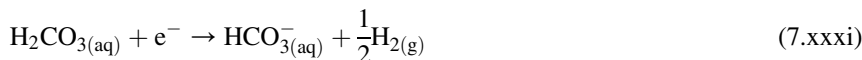
### 7.3.4 Effect of homogeneous reactions

As discussed earlier, it appears so far that the heterogeneous electrochemical reactions at the metal surface govern the rate of the  $\text{CO}_2$  corrosion. However, because these electrochemical reactions are heterogeneous surface processes, the rate of these reactions is defined by the concentration of the reactants at the metal surface (see Table 7.2), which is the reaction site, and can be very different from those in the bulk solution. In particular, the concentration of the so-called corrosive species (reactants of the cathodic reactions) at the metal surface may deplete if they are consumed at a faster rate than they are replenished. Ultimately, if the rate of consumption by the electrochemical reactions is sufficiently high, the process of supplying the reactants to the metal surface becomes the rate-determining step, and the so-called limiting current condition is reached. In  $\text{CO}_2$  corrosion, the limiting current is determined by two main processes, the homogeneous chemical reactions occurring in the solution adjacent to the metal surface and mass transfer from the the bulk solution.

The effect of homogeneous chemical reactions in the water/ $\text{CO}_2$  system on the rate of electrochemical reactions is probably the most important aspect of  $\text{CO}_2$  corrosion that differentiates the uniform  $\text{CO}_2$  corrosion from the corrosion induced by strong acids (e.g.,  $\text{HCl}$  or  $\text{H}_2\text{SO}_4$ ) or other weak acids, such as  $\text{H}_2\text{S}$  and organic acids. There are two major effects associated with homogeneous chemical reactions in  $\text{CO}_2$  corrosion:

1. The more significant effect is related to dissolved  $\text{CO}_2$  gas. Only  $\sim 0.2\%$  of dissolved  $\text{CO}_2$  molecules are hydrated to form  $\text{H}_2\text{CO}_3$  according to the hydration equilibrium (reaction 7.ii). This means that there is a large reservoir (buffer) of dissolved  $\text{CO}_2$  present in the solution to replenish the  $\text{H}_2\text{CO}_3$  concentration as it is consumed by dissociation and/or reduction at the steel surface. Therefore, in addition to mass transfer of  $\text{H}_2\text{CO}_3$  from the bulk solution, the limiting currents are increased as a result of this hydration reaction, occurring in the solution adjacent to the metal surface.
2. The second effect is associated with  $\text{H}_2\text{CO}_3$  and its generic buffering ability as a weak acid. Considering the  $\text{H}_2\text{CO}_3$  dissociation reaction (reaction 7.iii), the concentration of  $\text{H}^+$  at the metal surface is buffered when the equilibrium shifts toward the right-hand side (i.e., consumption of  $\text{H}^+$  by the reduction reaction). Although this does not influence the limiting current directly, it is of significance when discussing the mechanisms of charge transfer controlled corrosion at high  $\text{CO}_2$  partial pressures.

The exact mechanism of the cathodic reactions involved in  $\text{CO}_2$  corrosion, i.e., the sequence of electrochemical and chemical reactions, is a rather complex matter, in the sense that it involves a number of electroactive species that are interrelated through homogeneous chemical reactions. The arguments about the significance and the order of chemical and electrochemical reactions can be found in the literature dating back to 1970s. De Waard and Milliams, in their well-known study on prediction of  $\text{CO}_2$  corrosion rates [77], proposed a catalytic mechanism shown in reactions (7.xxxi) and (7.xxxii). The authors suggest that carbonic acid reduction (reaction 7.xxxi) is the predominant cathodic reaction. This reaction is succeeded by the association of the produced  $\text{HCO}_3^-$  and the  $\text{H}^+$  present in the solution, to replenish the carbonic acid concentration through a homogeneous chemical reaction (reaction 7.xxxii).



In 1977, Schmitt and Rothmann studied the effect of flow velocity and CO<sub>2</sub> partial pressure on the cathodic limiting current densities [78]. The authors suggested that the observed limiting currents in a CO<sub>2</sub>-saturated acidic solution is composed of a mass transfer component associated with H<sup>+</sup> and H<sub>2</sub>CO<sub>3</sub> and a chemical reaction component associated with a surface hydration of adsorbed CO<sub>2</sub>. Hence, it was hypothesized that the cathodic currents result from reduction of both H<sup>+</sup> and H<sub>2</sub>CO<sub>3</sub>, where the H<sup>+</sup> is supplied only through mass transfer from the bulk solution, whereas H<sub>2</sub>CO<sub>3</sub> is supplied both by mass transfer from bulk and by hydration of CO<sub>2</sub> at the metal surface [78].

Later in 1983, Więkowski et al. studied the CO<sub>2</sub> adsorption on electrodeposited iron electrodes using radiotracer method [68]. The authors reported no detectable adsorption of CO<sub>2</sub> on the metal surface. Considering these findings, Gray et al. in 1989, suggested that the CO<sub>2</sub> adsorption step in Schmitt and Rothmann's mechanism [78] is unnecessary for explaining the observed limiting currents [30]. Instead, the hydration reaction was considered a homogeneous reaction occurring in the solution near the metal surface. Using their proposed mechanism, the authors developed a mathematical model with iron dissolution as the anodic reaction and H<sup>+</sup>, H<sub>2</sub>CO<sub>3</sub>, and water reduction as the cathodic reactions. In their model, the surface concentration of H<sup>+</sup> was defined by mass transfer from the bulk, whereas for H<sub>2</sub>CO<sub>3</sub>, the surface concentration was defined by simultaneous consideration of the mass transfer and the preceding hydration reaction [30]. This study was further extended toward higher pH values in 1990 [15]. In the latter study, Gray et al. suggest that the reduction of HCO<sub>3</sub><sup>-</sup> ions also becomes significant at pH 6 and higher. In both studies, the experimental polarization curves were compared with the results from the model showing reasonable agreement, which further supported their proposed mechanism. The mechanism proposed by Gray et al. in these two studies [15,30] has become the most commonly accepted mechanism of CO<sub>2</sub> corrosion ever since, and has been used in numerous related studies.

The introduction of more comprehensive mathematical models in 1990s and early 2000s provided more insight into the influence of homogeneous reactions [71,72,79,80]. The key element in these models is the comprehensive consideration of the homogeneous chemical reactions at the vicinity of the electrode surface. The study by Turgoose et al. in 1992 was the first attempt to introduce one such model for the case of CO<sub>2</sub> corrosion [80]. Despite numerous simplifications and in some cases dubious assumptions, the authors were able to demonstrate the feasibility of this modeling approach. Considering the mass transfer limiting currents, the authors suggest that the previously proposed mechanisms by De Waard and Milliams [77,81] and Więkowski et al. [70] are only limited interpretations of numerous possibilities resulting from the complex CO<sub>2</sub> water chemistry in the vicinity of the metal surface. In particular, the authors suggested that the bicarbonate direct reduction is not necessarily required to explain the increased limiting currents in near-neutral CO<sub>2</sub>-saturated

solutions [80]. This approach was improved in the study by Pots [79], who developed a model for the calculation of limiting currents observed in CO<sub>2</sub>-saturated acidic solutions. The author reported similar results as Turgoose et al. [80], suggesting that the limiting currents can be adequately explained even if H<sub>2</sub>CO<sub>3</sub> was not considered an electroactive species [79]. As explained by the author, that is due to the local concentration of chemical species at the metal surface that may deviate significantly from the equilibrium at the bulk solution. Therefore, the homogeneous H<sub>2</sub>CO<sub>3</sub> dissociation near the metal surface, followed by electrochemical reduction of the produced H<sup>+</sup> ions, provides a parallel reaction pathway that is kinetically fast enough to result in the observed limiting currents [79].

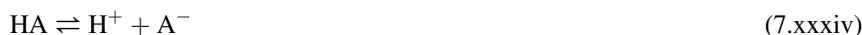
In a series of studies, Nešić et al. further improved this modeling approach by incorporating detailed water chemistry and charge transfer rate calculations [71,72,82–84]. The significance of the homogeneous chemical reactions in the solution near the metal surface was also emphasized by Nešić et al. [72]. The authors confirmed Pots' observation [79] that the limiting currents in CO<sub>2</sub>-saturated acidic solutions could be fully explained without requiring H<sub>2</sub>CO<sub>3</sub> to be electrochemically active. However, the authors also noted that the predicted corrosion rates were in better quantitative agreement with the experimental data when direct reduction of H<sub>2</sub>CO<sub>3</sub> was included in the model, but this mechanistic aspect was not further discussed [71,72].

It is important to notice that the more recent mechanistic arguments based on thorough consideration of the homogeneous chemical reactions are of significance, because they undermine the foundation of the commonly accepted mechanism, which is mainly based on the behavior of limiting current densities (e.g., the study of Schmitt and Rothmann [78] and Gray et al. [30,85]). Note that the initially proposed mechanisms by Schmitt and Rothmann [78] and Gray et al. [30,85] do not consider the possibility of preceding dissociation of carbonic acid for H<sup>+</sup> reduction reaction.

In 2008, Remita et al. set out to investigate the significance of H<sub>2</sub>CO<sub>3</sub> reduction reaction in CO<sub>2</sub>-saturated acidic solutions [58]. The authors developed a mathematical model similar to that of Nešić et al. [72] and formed a quantitative discussion by comparing the simulated polarization curves with experimental results. It was shown that the cathodic currents in CO<sub>2</sub>-saturated solution at pH 4 can be reasonably explained through H<sup>+</sup> reduction reaction alone [58]. The authors claimed that H<sub>2</sub>CO<sub>3</sub> reduction is therefore insignificant in CO<sub>2</sub> corrosion. However, considering the limited experimental range (pH 4 and 1 bar CO<sub>2</sub>), where the cathodic currents are mostly under mass transfer influence (as shown in the data reported by Nešić et al. [29]), and the concentration of H<sub>2</sub>CO<sub>3</sub> is low (less than 10<sup>-4</sup>), it is unrealistic to generalize the observations reported in this study [58]. Note that, as discussed in earlier studies, the limiting currents are identical whether H<sub>2</sub>CO<sub>3</sub> was considered electroactive or not.

This reaction sequence (i.e., H<sub>2</sub>CO<sub>3</sub> dissociation followed by H<sup>+</sup> reduction) is now known in the literature as the “buffering effect” mechanism. It needs to be clearly distinguished from the “direct reduction” mechanism described earlier. Such mechanistic discussions are not particular for CO<sub>2</sub> corrosion, as similar arguments have been put forward for various weak acids, such as acetic acid and hydrogen sulfide [56,57,86,87]. Considering a generic weak acid, HA (e.g., H<sub>2</sub>CO<sub>3</sub>, HCO<sub>3</sub><sup>-</sup>, H<sub>2</sub>S, HAc),

its direct reduction can be expressed as reaction (7.xxxiii). As a weak acid that is only partially dissociated in the solution, HA is also involved in homogeneous chemical equilibrium described as reaction (7.xxxiv). In addition, in acidic solutions, the H<sup>+</sup> reduction reaction occurs as shown in reaction (7.xxxv).



The “direct reduction” mechanism suggests that HA reduction (reaction 7.xxxiii) is significant; therefore the cathodic currents in acidic solutions are the result of two electrochemical reactions, HA reduction and H<sup>+</sup> reduction. On the other hand, the “buffering effect” mechanism suggests that, reaction (7.xxxiii), the reduction of HA, is insignificant as compared to reaction (7.xxxv), the reduction of H<sup>+</sup>. Therefore, the dominant cathodic reaction in acidic solutions is H<sup>+</sup> reduction, while HA buffers the concentration of H<sup>+</sup> ions at the surface through the homogeneous reaction (7.xxxiv).

These two mechanisms may be qualitatively distinguished by studying the behavior of charge transfer controlled cathodic currents [57,86]. If the concentration of the common reactant between the two possible mechanisms (H<sup>+</sup>) is kept constant, each mechanism shows a distinct behavior as the concentration of the weak acid is increased (Fig. 7.2) [86]. For the case of the “buffering effect” mechanism, no significant change in charge transfer controlled currents is expected, because the weak acid is not electrochemically active. On the other hand, for the “direct reduction” mechanism the charge transfer controlled cathodic currents are increased as the concentration of the reactant (the weak acid) is increased. Note that the magnitudes of the limiting current in both mechanisms are identical. In addition, as shown in Fig. 7.2(a), in certain conditions a secondary limiting current wave may also be observed in the case of “direct reduction” mechanism.

Examples for both mechanisms at play are available from experimentation, as shown in Fig. 7.3. In Fig. 7.3(a) it is demonstrated that H<sub>2</sub>S follows the direct reduction mechanism with a clear secondary limiting current observed at moderate and high H<sub>2</sub>S concentrations [56]. On the other hand, the buffering effect mechanism was shown to be the dominant reaction pathway in the case of acetic acid reduction (Fig. 7.3(b)), where no significant change in charge transfer controlled currents were observed with acetic acid (HAc) concentrations up to 500 mass ppm [86].

Considering the possibilities of the “direct reduction” and “buffering effect” mechanisms, Tran et al. focused on the study of the H<sub>2</sub>CO<sub>3</sub> reduction reaction [88]. The authors noted that, even at higher CO<sub>2</sub> partial pressures the pure charge transfer controlled cathodic currents are not clearly observed on an X65 mild steel surface and that this hypothetical behavior cannot be easily verified. Therefore, the stainless

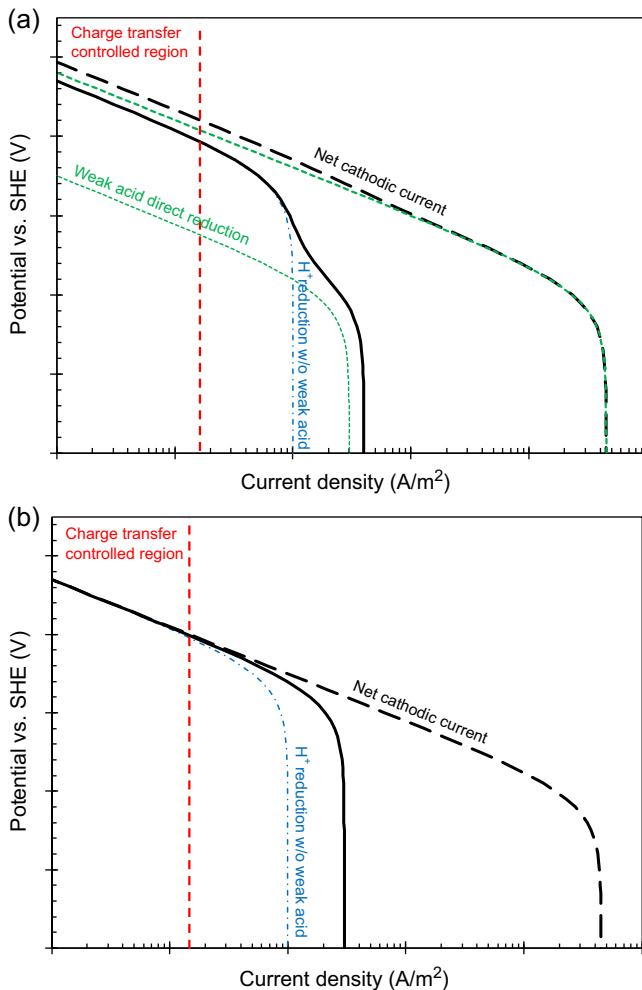


**Figure 7.2** Hypothetical cathodic steady state voltammograms at a constant pH and two different concentrations of a weak acid (*solid black line* < *dashed black line*). *Black lines*: net current, *dotted-dashed blue lines*:  $H^+$  reduction without weak acid present, and *dashed green lines*: weak acid direct reduction. (a) Direct reduction mechanism and (b) buffering effect mechanism. SHE, standard hydrogen electrode.

steel electrodes, being a nobler substrate, was used to eliminate the interference by the anodic iron dissolution reaction. By comparing the steady-state voltammograms for pH 4 and pH 5 at 1 and 10 bar  $CO_2$  partial pressures, the authors reported a behavior resembling that shown in Fig. 7.2(b) and hence concluded that the cathodic currents in  $CO_2$ -saturated solutions follow the “buffering effect” mechanism [88]. However, considering the effect of alloying compounds of stainless steel ( $\sim 20$  wt% Cr and 10 wt% Ni) and their corresponding passive films, on the electroactivity of the metal

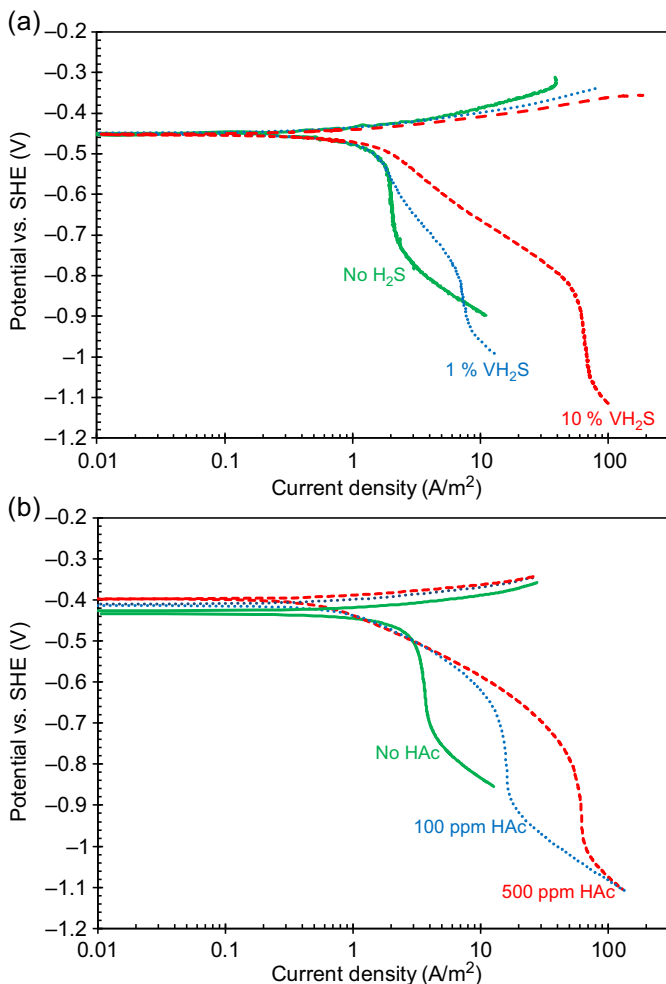


**Figure 7.3** Polarization behavior of X65-API mild steel at pH 4 and 30°C (86°F). (a) H<sub>2</sub>S system with total pressure = 1 bar (14.5 psi), 1000 rpm rotating cylinder electrode and various pH<sub>2</sub>S expressed in volume percent. (b) Acetic acid (HAc) system at 2000 rpm rotating disk electrode and various total HAc concentrations expressed in mass fraction. *SHE*, standard hydrogen electrode.

(a) Data taken from Y. Zheng, B. Brown, S. Nešić, Electrochemical study and modeling of H<sub>2</sub>S corrosion of mild steel, *Corrosion* 70 (2014) 351–365. (b) Data taken from A. Kahyarian, B. Brown, S. Nesic, Mechanism of cathodic reactions in acetic acid corrosion of iron and mild steel, *Corrosion* 72 (2016) 1539–1546.

surface, the observed mechanism for cathodic currents cannot be applied to mild steel without further verifications.

The discussion in this section shows a continuous development in understanding the fundamental mechanism of cathodic reactions involved in CO<sub>2</sub> corrosion over the years. Despite that, there are still various important aspects that remain

controversial and require further investigations. The effect of CO<sub>2</sub> and carbonated species on the mechanism of iron dissolution reaction, the electrochemical mechanism of hydrogen evolution reactions, and the significance of direct H<sub>2</sub>CO<sub>3</sub> and HCO<sub>3</sub><sup>-</sup> reduction are among the subjects that require further elucidation.

### 7.3.5 Effect of mass transfer

In CO<sub>2</sub> corrosion, in addition to the homogeneous chemical reactions as discussed in Section 7.3.4, the mass transfer from the bulk solution is another process replenishing the concentration of the corrosive species at the metal surface as they are consumed in the corrosion process. The importance of mass transfer is acknowledged in many studies [89–92]. For example, Fig. 7.4 demonstrates the effect of fluid velocity on the observed corrosion rates at 1 bar (14.5 psi) CO<sub>2</sub> and various pH values. The increase of corrosion rate by increasing the fluid velocity suggests that corrosion currents are under mass transfer influence at this specific conditions. However, the effect of the fluid velocity on the corrosion rate may decrease, if the solution is highly buffered (e.g., high CO<sub>2</sub> partial pressure (P<sub>CO<sub>2</sub></sub> > 10 bar(145 psi)) [93], or in the presence of organic acids [67]). In such conditions the limiting current is significantly increased by the high rate of the chemical reactions and the corrosion rate is controlled by the rate of electrochemical reactions, which are not influence by the mass transfer rate.

The mass transfer in a corroding system consists of a molecular diffusion component, induced by the concentration gradient of the chemical species; an electromigration component, as the result of ionic movement in the presence of an electric field; and a convective flow component due to the movement of the bulk solution. The flux of each chemical species (*i*) involved in the corrosion process may therefore be expressed through the well-known Nernst–Planck equation:

$$N_i = -D_i \nabla C_i - z_i u_i F C_i \nabla \phi + v C_i \quad (7.4)$$

The term “ $vC_i$ ” represents the convective flow toward the metal surface. In turbulent flow regime, commonly observed in transmission pipelines, turbulent mixing dominates the bulk movement of the fluid and can be characterized in terms of eddy diffusivity and lumped in with the molecular diffusion term.

Considering the typical conditions of CO<sub>2</sub> corrosion, Eq. (7.4) can be simplified by assuming the electromigration term is negligible. This assumption is valid in free corroding, nonpolarized systems with sufficient ionic strength, where the potential gradient inside the solution ( $\nabla \phi$ ) is small. In its simplest form, the flux of chemical species can be described by the mass transfer coefficient ( $k_m$ ) as shown in Eq. (7.5), where the mass transfer coefficient can be expressed in terms of the dimensionless Sherwood number ( $Sh$ ) in Eq. (7.6).

$$N_i = k_m (C^b - C^s) \quad (7.5)$$

$$k_m = \frac{ShD}{L} \quad (7.6)$$

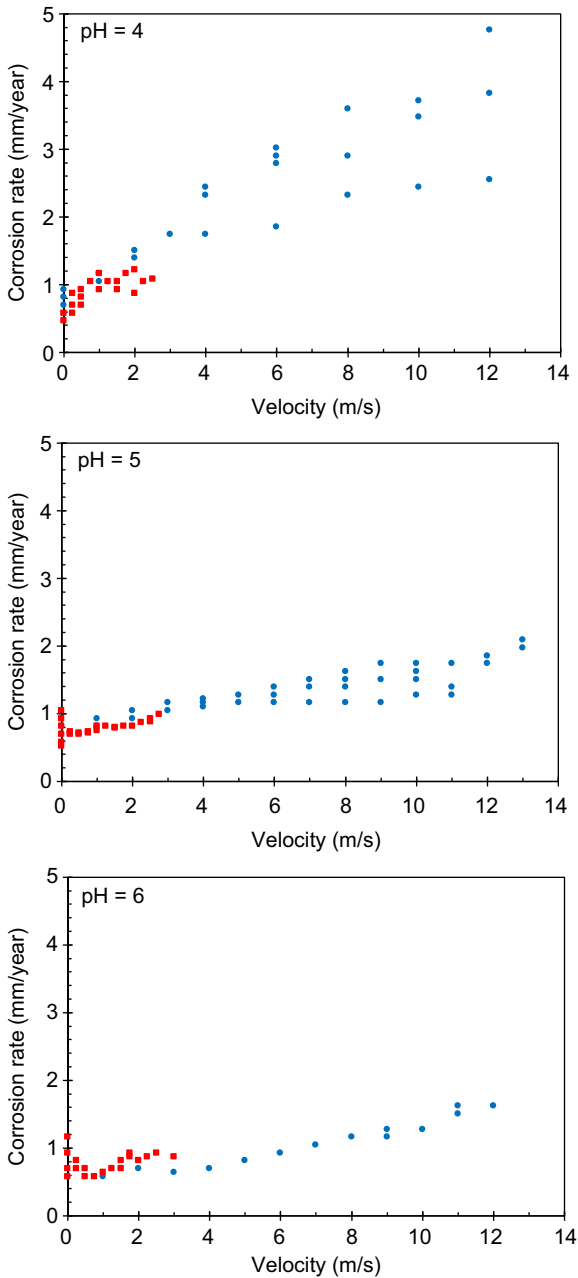


**Figure 7.4** Effect of flow velocity on corrosion rate at 1 bar (14.5 psi) CO<sub>2</sub>, 20°C (68°F), 1 wt% NaCl, and different pH values. *Blue circles*: pipe flow (15 mm ID), *red squares*: rotating cylinder (10 mm OD).

Data taken from S. Netic, G.T. Solvi, J. Enerhaug, Comparison of the rotating cylinder and pipe flow tests for flow-sensitive carbon dioxide corrosion, *Corrosion* 51 (1995) 773–787.

The mass transfer coefficients for various flow regimes and geometries have been extensively studied. For the turbulent flow around a rotating cylinder electrode, the correlation of Eisenberg et al. [94] or other similar correlations can be used [95]. The mass transfer correlation in fully developed turbulent flow through smooth, straight pipes was defined by Berger and Hau [96]. For other conditions such as multi-phase flow and flow around U-bends and elbows, similar correlations can also be readily found in the literature [97–101].

For an electrochemical reaction at steady state, the rate at which the electroactive species are transferred toward/away from the surface is equal to the rate of the charge transfer reaction at the surface. Therefore, the current density can also be expressed in terms of mass transfer via Eq. (7.7).

$$i = nFk_m(C^b - C^s) \quad (7.7)$$

In Eq. (7.7)  $C^b$  and  $C^s$  are the concentrations of the electroactive species in the bulk solution and at the metal surface, respectively. The value of  $C^s$  appearing in Eq. (7.7) and the current/potential relationships of Table 7.3 are generally unknown. However, for a first-order electrochemical reaction it can be shown that:

$$\frac{1}{i} = \frac{1}{i_{ct}} + \frac{1}{i_{lim}} \quad (7.8)$$

The  $i_{ct}$  term in Eq. (7.8) is the charge transfer controlled current, when the electrochemical reaction is proceeding without any mass transfer resistance, and it can be calculated as discussed in Section 7.3.3 knowing that  $C^s = C^b$ . The  $i_{lim}$  is the mass transfer limiting current that is defined by Eq. (7.7) when  $C^s = 0$ .

For an electrochemical reaction preceding a chemical reaction, such as  $H_2CO_3$  reduction that follows the  $CO_2$  hydration reaction, the limiting current is a combination of mass transfer and the chemical reaction and is obtained by simultaneous consideration of both processes. A composite limiting current calculation for  $H_2CO_3$  reduction on a rotating disk electrode was implemented in the model developed by Gray et al. [15,30], and it is described in detail elsewhere [102]. Similar theoretical calculations for turbulent flow regimes of rotating cylinder electrode and straight pipe flow were developed and implemented by Nešić et al. [103,104]. The mathematical expression developed by Nešić et al. is shown in Eq. (7.9) [103]. In a sense, this equation is the chemical reaction limiting current multiplied by a correction factor (the  $\coth(\delta_d/\delta_r)$  term) to account for the effect of turbulent mixing.

$$i_{lim,H_2CO_3} = n_{H_2CO_3} F C_{H_2CO_3}^b (Dk_{b,hyd})^{1/2} \coth \frac{\delta_d}{\delta_r} \quad (7.9)$$

$$\delta_d = D/k_m \quad (7.10)$$

$$\delta_r = (D/k_{b,hyd})^{1/2} \quad (7.11)$$

The CO<sub>2</sub> corrosion of mild steel is also often accompanied by the formation of a corrosion product layer. The deposited corrosion product on the steel surface can be characterized as a solid porous layer that acts as an additional mass transfer barrier. In this case, the limiting current appearing in Eq. (7.8) can be calculated using a composite mass transfer coefficient to account both for the flow effect and the resistance caused by the corrosion product layer. This composite mass transfer coefficient follows Eq. (7.12), where  $k_m$  is the mass transfer coefficient due to the flow, as shown in Eq. (7.5), and  $k_d$  is the mass transfer coefficient inside the porous layer.

$$\frac{1}{k_{\text{comp.}}} = \frac{1}{k_m} + \frac{1}{k_d} \quad (7.12)$$

The mass transfer coefficient inside the corrosion product layer,  $k_d$ , can be quantified as diffusion through a porous medium:

$$k_d = \frac{\varepsilon \tau D}{\delta_l} \quad (7.13)$$

In Eq. (7.13), the  $\varepsilon$  and  $\tau$  terms are porosity and tortuosity of the corrosion product layer, respectively,  $D$  is the diffusion coefficient, and  $\delta_l$  is the corrosion product layer thickness. In addition to decreasing the mass transfer of the corrosive species to the surface, the solid corrosion product layers impede corrosion also by covering/blocking the steel surface at locations where they are attached, making them unavailable for electrochemical reactions (see Fig. 7.5). A more detailed description of the corrosion product layers is given in the following chapter.

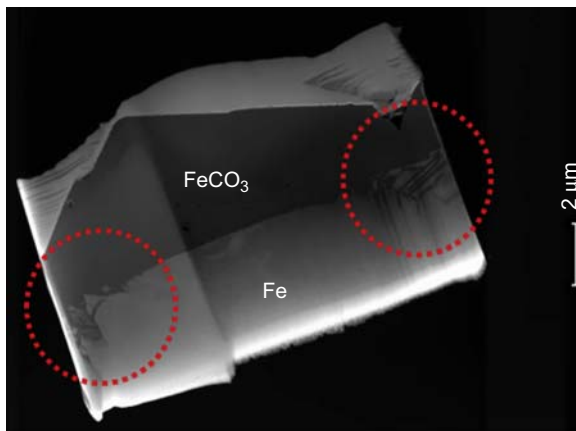


**Figure 7.5** A transmission electron microscope image of mild steel surface with iron carbonate corrosion product layer. Little corrosion is seen at locations where iron carbonate is attached to the steel surface with most of the attack happening in the highlighted area between iron carbonate grains.

Adapted from Jiabin Han, Galvanic Mechanism of Localized Corrosion for Mild Steel in Carbon Dioxide Environments (Doctoral dissertation), Ohio University, 2009.

## 7.4 Corrosion product layers

In  $\text{CO}_2$  corrosion, one almost always encounters formation of corrosion product layers. These will typically be made up of one or more of the following compounds:

- iron carbide (cementite)
- iron carbonate (siderite)
- iron oxide (magnetite)

### 7.4.1 Iron carbide ( $\text{Fe}_3\text{C}$ )

Iron carbide ( $\text{Fe}_3\text{C}$ ) is often labeled as the uncorroded portion of the steel. It is primarily associated with mild steels having a high carbon content and a ferritic-pearlitic microstructure. During corrosion of such steel, the ferrite phase dissolves and a porous iron carbide network is exposed (see Fig. 7.6). Given that iron carbide is an electronic conductor, this porous network serves as an additional cathodic surface for reduction of corrosive species, which would lead to an increase in the corrosion rate. On the other

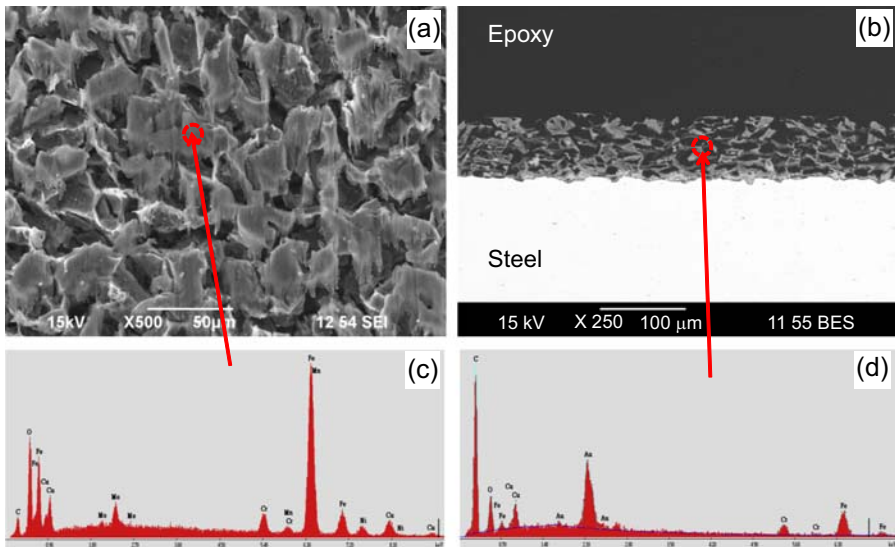


**Figure 7.6** A cross-section of a mild steel specimen after 41 h of exposure in a 3 wt% NaCl aqueous solution,  $80^\circ\text{C}$  ( $176^\circ\text{F}$ ), pH 6,  $\text{pCO}_2 = 1$  bar (14.5 psi). Scanning electron microscopy images of the (a) top view showing the iron carbide network, (b) cross-section view, and (c) and (d) the respective energy dispersive spectroscopy spectrum [105].

Reproduced with permission from NACE International, Houston, TX. All rights reserved.

hand, it also presents an additional diffusion barrier, making it harder for the corrosive species to reach the steel surface, which would lead to a slight decrease in the corrosion rate. The porous iron carbide network also makes it harder for the ferrous ions to diffuse away into the bulk solution, enhancing their buildup at the steel surface. With other conditions being favorable (e.g., elevated temperature) this may lead to precipitation of protective iron carbonate within the pores of the iron carbide corrosion product layer (discussed later), dramatically decreasing the corrosion rate (see Fig. 7.7). Finally, the porous iron carbide corrosion product layer can also impede organic corrosion inhibitors from adsorbing on the underlying steel surface, although how and why this happens is not properly understood. Owing to this multitude of opposing effects, the overall influence of iron carbide corrosion product layers on CO<sub>2</sub> corrosion of mild steel is often simply ignored; however, research is underway to further qualify and quantify these effects.

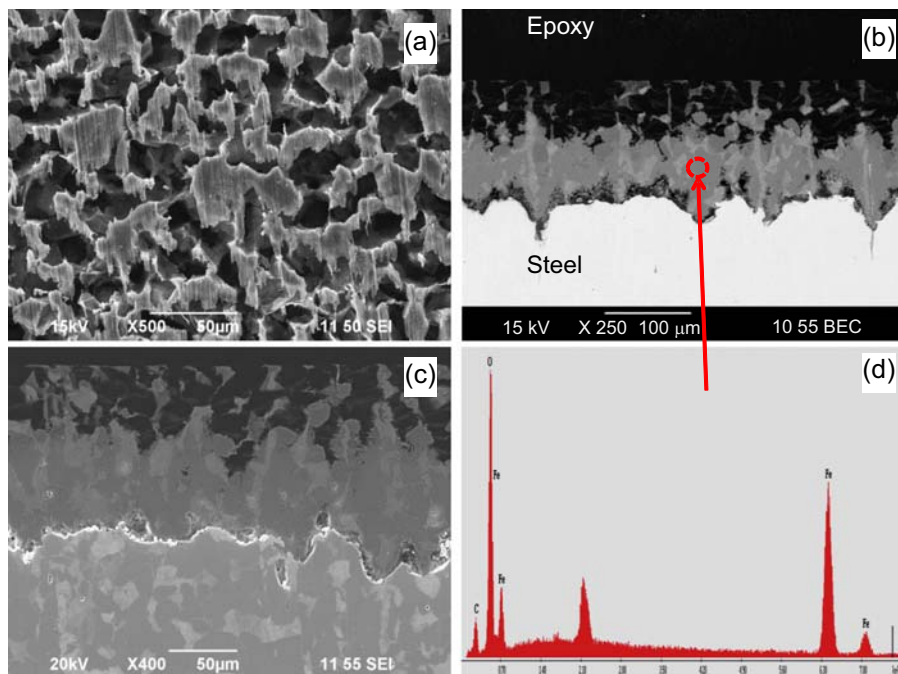


**Figure 7.7** A cross-section of a mild steel specimen after 90 h of exposure in a 3 wt% NaCl aqueous solution, 80°C (176°F), pH 6,  $p\text{CO}_2 = 1$  bar (14.5psi). Scanning electron microscopy images of the (a) top view showing the iron carbide network, (b) cross-section view, and (c) and (d) the respective energy dispersive spectroscopy spectrum. The steel surface cross-section (c) was etched with 2% Nital [105].

Reproduced with permission from NACE International, Houston, TX. All rights reserved.

### 7.4.2 Iron carbonate ( $\text{FeCO}_3$ )

When the buildup of ferrous ions in the  $\text{CO}_2$  aqueous solution exceeds the solubility of iron carbonate, it will precipitate according to reaction (7.xxxvi).



As discussed earlier, a porous iron carbonate corrosion product layer formed on the steel surface can slow down the corrosion process by presenting a diffusion barrier for the species involved in the corrosion process and by covering/blocking a portion of the steel surface and protecting it from corrosion.

Iron carbonate corrosion product layer morphology and its protectiveness strongly depend on the precipitation rate. The other important factor is corrosion of the underlying steel surface, which continuously “undermines” the iron carbonate layer. As voids are being created by corrosion, they are filled by the ongoing precipitation, with the final morphology and ultimately its protectiveness hanging in the balance. When the rate of precipitation largely exceeds the rate of undermining by corrosion, a dense well-attached and protective layer forms, sometimes very thin ( $\sim 1\text{--}10\ \mu\text{m}$ ) but still protective (see Fig. 7.8). Vice versa, when the corrosion process undermines the newly formed scale faster than precipitation can fill in the voids, a porous and unprotective layer forms, which can sometimes be very thick ( $\sim 10\ \text{m--}100\ \mu\text{m}$ ) and still be unprotective. Therefore, it is not the thickness and overall appearance of the iron carbonate layer that are best indicators of its protectiveness, rather it is the density and particularly the degree of attachment to the steel surface that are dominant.

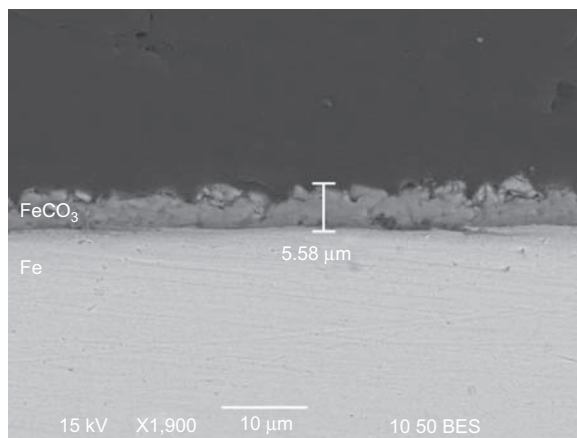


**Figure 7.8** Scanning electron microscopy images of a cross-section of a mild steel specimen after 72 h of exposure in a 3 wt% NaCl aqueous solution,  $80^\circ\text{C}$  ( $176^\circ\text{F}$ ), pH 6.6,  $p\text{CO}_2 = 0.5\ \text{bar}$  (7.25 psi), showing a thin and protective iron carbonate corrosion product layer.

Many factors affect the formation of iron carbonate corrosion product layers. The most important one is water chemistry, and the concept of supersaturation, which is defined as:

$$S_{\text{FeCO}_3} = \frac{C_{\text{Fe}^{2+}} C_{\text{CO}_3^{2-}}}{K_{\text{sp}}} \quad (7.14)$$

where  $K_{\text{sp}}$  is the iron carbonate dissolution equilibrium constant [106]. Owing to the relatively slow kinetics of iron carbonate precipitation, supersaturation with respect to iron carbonate has to be greatly exceeded (by a factor of 10–100) to form a protective iron carbonate layer. This usually happens at high pH, which is a key precondition for protective iron carbonate layer formation ( $\text{pH} > 6$ ). It should be pointed out that this refers to the pH at the steel surface where precipitation happens, which is always higher than pH in the bulk, often by a whole pH unit or even two, particularly in the presence of other types of diffusion barriers such as iron carbide layers described earlier. Temperature is another very important factor. At room temperature, the process of iron carbonate precipitation is very slow and unprotective layers invariably form, even at very high supersaturation values. Conversely, at higher temperatures [ $T > 60^\circ\text{C}$  ( $140^\circ\text{F}$ )] precipitation proceeds rapidly enough to yield dense, well-attached, and very protective surface layers, even at low supersaturation.

### 7.4.3 Iron oxide ( $\text{Fe}_3\text{O}_4$ )

At even higher temperatures [ $T > 100^\circ\text{C}$  ( $212^\circ\text{F}$ )] iron oxide (magnetite) will form in CO<sub>2</sub> aqueous solutions. When thermodynamic conditions are favorable for the formation of magnetite (high pH and high temperature), it appears rapidly, forming a very

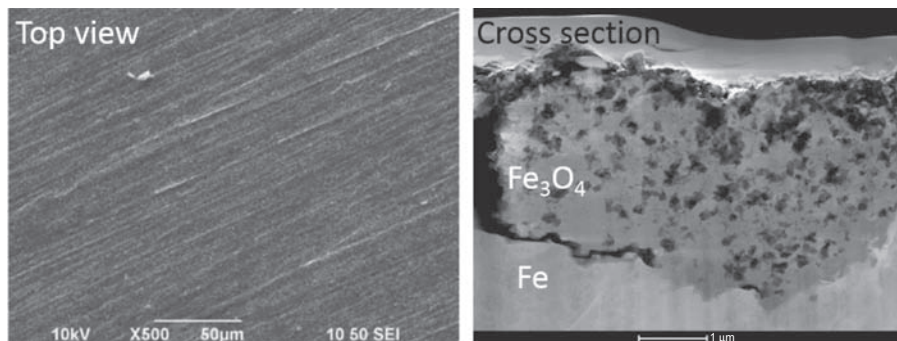


**Figure 7.9** Scanning electron microscopy image of the top surface and transmission electron microscopy image of the cross-section of steel surface exposed for 4 days at  $200^\circ\text{C}$  ( $392^\circ\text{F}$ ),  $\text{pCO}_2 = 1$  bar (14.5 psi) at  $25^\circ\text{C}$  ( $77^\circ\text{F}$ ), 1 wt% NaCl.

Reproduced with permission from Tanaporn Tanupabrunsun, Thermodynamics and Kinetics of Carbon Dioxide Corrosion of Mild Steel at Elevated Temperatures (Doctoral dissertation), Ohio University, 2013.

thin ( $\sim 1 \mu\text{m}$ ) and very protective layer, tightly adhering to the steel surface (see Fig. 7.9). When a magnetite layer forms, the corrosion rates typically decrease by one order of magnitude or more. Actually, there are indications that some magnetite forms even at temperatures lower than  $100^\circ\text{C}$  ( $212^\circ\text{F}$ ) and is often very hard to detect as it appears in small quantities in cavities and pores of the iron carbonate corrosion product layer, contributing to overall protectiveness.

Other salts can precipitate to form even more complex surface layers that may affect the corrosion rate. The most important are iron sulfides, which form in  $\text{H}_2\text{S}$ -containing aqueous solutions, covered elsewhere in this monograph. Scales containing calcium carbonate, barium sulfate etc., may form in environments containing formation water, also affecting the protectiveness of surface layers [107]. A more complete analysis of scaling and factors that affect it is beyond the scope of the present review.

## 7.5 Additional aqueous species

The  $\text{CO}_2$  corrosion is often complicated by the presence of additional aqueous species. Most important examples are:

- Organic acids
- Hydrogen sulfide
- Chlorides

### 7.5.1 Organic acids

The first reports on the effect of organic acid in  $\text{CO}_2$  corrosion of mild steel appeared in the 1940s, where it was shown that even concentrations as low as 300 ppm can cause severe corrosion of pipeline steel [108]. A number of low-molecular-weight, water-soluble, organic/carboxylic acids are found in oil-field brines, such as formic acid ( $\text{HCOOH}$ ) and propionic acid ( $\text{CH}_3\text{CH}_2\text{COOH}$ ); however, acetic acid ( $\text{CH}_3\text{COOH}$  or shortly  $\text{HAc}$ ) is by far the most prevalent organic acid causing corrosion problems for mild steel. In 1983, Crolet and Bonis reported that the presence of  $\text{HAc}$  in the brine increased the corrosion rate of mild steel significantly [109]. Subsequently, carbon dioxide corrosion in the presence of acetic acid has been the subject of numerous studies. These include laboratory investigations in model systems using electrochemical methods, such as cyclic voltammetry [110,111], potentiodynamic sweeps [86,112,113], electrochemical impedance spectroscopy [114,115], as well as corrosion experiments using field brines [109,116,117]. The detrimental effect of acetic acid was primarily seen at high temperatures ( $>50^\circ\text{C}$ ) and in the lower pH range (pH 3.5–5.0). Similar to carbonic acid,  $\text{HAc}$  is also a weak, partially dissociated acid, according to reaction (7.xxxvii).



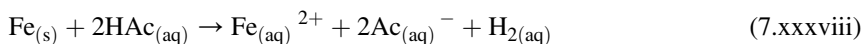
The pH determines the distribution of the acetic species in the solution, as shown in Table 7.5 for a typical pH range of oil-field brines. Clearly, at pH 4, corresponding to a pure water/ $\text{CO}_2$  system seen, for example, in condensed water, most of the acetic

**Table 7.5 Acetic acid species distribution at various pH values at 80°C (176°F)**

pH	[HAc]/mol%	[Ac <sup>-</sup> ]/mol%
4	88	12
5	42	58
6	6.8	93.2
6.6	1.8	98.2

species are in the form of undissociated acid. The opposite is true at pH 6.6, typical for heavily buffered brines, where most of the acetic species are in the form of acetate ion.

Similar to the case of carbonic acid corrosion, the mechanism of acetic acid corrosion has been intensely debated in the last 2 decades. Although many studies suggest that the increased corrosion rates in the presence of acetic acid is due to its direct reduction at the metal surface [32,111,115,118–121], others suggest that acetic acid corrosion follows the buffering effect mechanism [57,67,122,123]. It has now been established that the buffering effect is dominant [57,86] and that the most influential factor is the concentration of the undissociated (“free”) acetic acid and not the acetate ion. Therefore, one can appreciate that the organic acids are a major corrosion concern primarily at lower pH values [114,124]. The overall corrosion reaction due to acetic acid can be written as reaction (7.xxxviii).



Another aspect of the acetic acid effect is related to how it affects protective corrosion product layers typically found on the steel surface exposed to aqueous CO<sub>2</sub> solutions. Iron acetate is very soluble and is not found as a solid deposit on the steel surface in the pH range of interest in the oil and gas industry. However, iron carbonate, which is often present, can be protective as described earlier. There seems to be an interaction where acetic acid leads to destabilization of protective iron carbonate layers that may result in localized attack, although the mechanism is not known clearly [122,125–127]. This is the subject of some ongoing investigations.

### 7.5.2 Hydrogen sulfide

Corrosion of mild steel in the presence of aqueous hydrogen sulfide (H<sub>2</sub>S) has also been extensively investigated in the last few decades [56,59,60,74,87]. Aqueous H<sub>2</sub>S is another weak acid that affects the speciation and is directly involved with the electrochemical reactions at the steel surface. It was confirmed that hydrogen sulfide follows the direct reduction mechanism (see Section 7.3.4) [56,59,60]. A number of different solid iron sulfides can form as corrosion product layers, some of which are protective. This topic is covered in a separate chapter in the present monograph and will not be discussed here any further.

### 7.5.3 Chlorides

A very common species found in oil-field brines is the aqueous chloride ( $\text{Cl}^-$ ) anion, which can be present anywhere from a fraction of a percent to over 10% by weight. Chlorides are generally considered to be detrimental in  $\text{CO}_2$  corrosion of mild steel and are often lumped in with aqueous  $\text{CO}_2$ , organic acids, and  $\text{H}_2\text{S}$ , even if they are neither acidic species nor electroactive. Many of the arguments about the detrimental effect of chlorides are either purely circumstantial or are blindly transposed from systems involving stainless steel corroding in aerated solutions, which is clearly inadequate. Actually, it was shown that uniform  $\text{CO}_2$  corrosion rate of mild steel significantly decreases with an increase of chloride concentration (above a few wt%) [128,129]. This is due to a retardation of homogenous physicochemical processes underlying corrosion, such as diffusion and chemical reactions, occurring in nonideal solutions loaded with chlorides.

On the other hand, the presence of chlorides increases electrical conductivity of the solution, and in the case of nonideal solutions, it increases the solubility of solid corrosion products. This has been thought to be the reason for failure of protective iron carbonate corrosion product layers and localized corrosion in brines with high chloride concentrations. However, it is still not clear if this effect is specific to chlorides or is a generic effect caused by nonideality and high conductivity of the electrolyte.

## 7.6 Multiphase flow effects

In the field,  $\text{CO}_2$  corrosion almost always happens in flowing solutions and often in the context of multiphase flow. Multiphase flow can be defined as the concurrent flow of substances having two or more *phases*. A *phase* refers to a state of a substance, such as gas, liquid, or solid. The term *multiphase flow* is used also to refer to the concurrent flow of two or more substances that are of the same phase but do not mix and are either present as continuous or dispersed in the other [130]. In pipes, a variety of multiphase flow patterns may arise [131]. These flow patterns are often represented as bounded areas in a two-dimensional graph, termed a *flow pattern map* or *flow regime map*. An example of a flow pattern map is given in Fig. 7.10. The boundaries on the map are the transition lines, which are a function of flow rates, fluid physical properties, and pipe orientation [132].

Theoretically, there are two main ways that flow may affect  $\text{CO}_2$  corrosion of mild steel: through *mass transfer* or via *mechanical means*. Turbulent flow enhances mass transport of species to and away from the steel surface by affecting transport through the boundary layer as described in Section 7.3.5. It has been argued that mass transfer often plays a relatively small role, as the  $\text{CO}_2$  corrosion rate is often controlled by charge transfer or is limited by a slow chemical  $\text{CO}_2$  hydration step, or is controlled by a protective corrosion product layer, as mentioned in Section 7.3. On the other hand, intense flow could theoretically lead to mechanical damage of protective iron carbonate corrosion product layers or inhibitor films. Both these mechanisms are aggravated by flow disturbances, such as valves, constrictions, expansions, and bends,

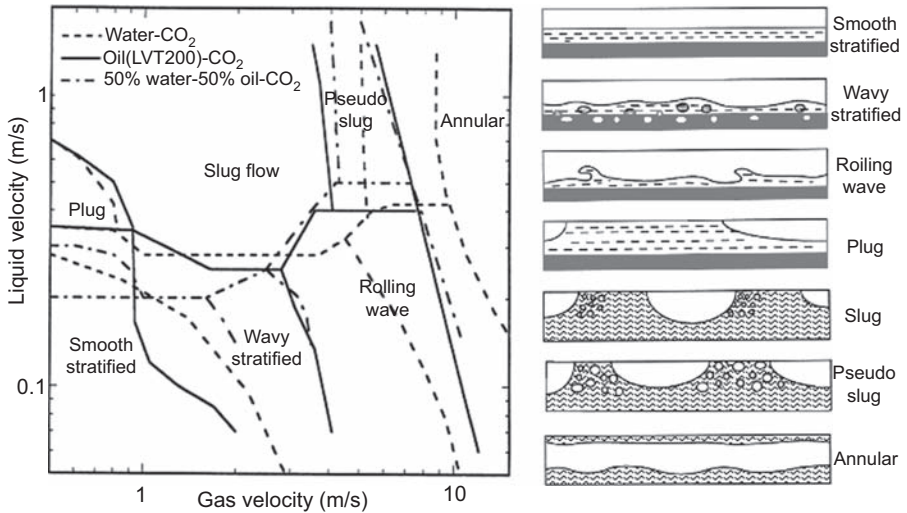


**Figure 7.10** Three-phase flow patterns and flow pattern map. Transitions for two-phase flow were included in the map for comparison.

Reprint with permission from K. Kee, A Study of Flow Patterns and Surface Wetting in Gas-Oil-Water Flow (Doctoral dissertation), Ohio University, 2014.

where a local increase of near-wall turbulence is seen. The same is true for some multiphase flow regimes, which are commonplace in the field.

When it comes to the mechanical effects of flow on corrosion, the wall shear stress (WSS) has often been used as the relevant parameter to characterize this interaction. The operating hypothesis was that at some sufficiently high WSS the hydrodynamic forces at the corroding steel surface may lead to mechanical damage of the protective corrosion product layers or inhibitor films.

In single-phase liquid flow, the WSS can be readily calculated and is typically of the order of 1–10 Pa. In horizontal two-phase gas–liquid flow, laboratory investigations at atmospheric conditions have shown that the maximum WSS is of the order of 100 Pa, obtained in the slug flow regime [133]. Using mathematical modeling, it is estimated that the highest practical wall shear stress that could be expected in multiphase flow seen in the field is of the order of 1000 Pa [133]. These values are several orders of magnitude lower than the reported adhesion strength of inhibitor films or protective iron carbonate layers, which are of the order of  $10^6$  Pa or even higher [133–136]. This suggests that mechanical removal of protective films or layers solely by mechanical forces (WSS) typically seen in the field is very unlikely. The only exception are some very specific multiphase flow conditions that lead to cavitation or droplet impingement, when very large short-lived hydrodynamic stress fluctuations at the pipe wall are seen that can damage the protective inhibitor films and corrosion product layers, leading to localized attack. Even in those cases, using excess corrosion inhibition makes it possible to overcome the problem [137].

Another very important feature of multiphase flow is related to the so-called water wetting. Internal corrosion in pipelines occurs only if the water phase wets the internal

steel surface, a condition termed *water wetting*. When oil is in contact with the internal pipe surface, a scenario called *oil wetting*, corrosion cannot occur. The multiphase flow factors that lead to one or the other scenario are primarily water cut (amount of water), flow regime, and pipe orientation [138,139]. These factors influence the physical distribution of fluids across the pipe cross-section and across the length of the pipeline. Another factor that affects water wetting is wettability (ability to wet a surface), which is a function of the state of the steel surface and the chemical compositions of the aqueous and hydrocarbon phases. Stable water wetting is most often encountered in horizontal oil–water and oil–water–gas multiphase flow. At a low flow rate, the water flows separately as a continuous phase at the bottom of the line and can lead to corrosion. As the flow rate increases, and the main flow gains sufficient turbulence, this leads to gradual water entrainment and a transition to oil wetting, decreasing the likelihood of corrosion. However, even at high flow rates, when most of the water is entrained, it is possible to have water accumulate at low spots in the line, leading to corrosion.

The presence of solids, such as produced sand, and other inorganic and organic solid matter further complicates the effects of multiphase flow on corrosion. At high flow rates, the entrained solids may impinge on the internal pipe wall and lead to mechanical removal of any protective layer and, in extreme cases, the erosion of the underlying steel itself. This effect is particularly pronounced at flow disturbances, such as tees, valves, bends, constrictions, and expansions, and in intermittent flow patterns, such as slug and churn flow [140,141]. At the other end of the spectrum, at very low flow rates, settling of solids may occur, leading to so-called under-deposit corrosion [142,143]. Under-deposit corrosion becomes an issue when corrosion inhibitors are unable to penetrate through the solids and cannot protect the surface covered by the porous layer of solids, or when this layer leads to initiation of microbiologically induced corrosion.

Dewing corrosion often termed *top-of-line-corrosion* (TLC) occurs in wet gas pipelines, when there is a significant temperature difference between the transported fluids and the outside environment. When the gas/liquid flow is stratified, saturated water vapor condenses and forms water droplets on the side and the top of the internal walls of the pipeline. These quickly become saturated with acid gases ( $\text{CO}_2$ ,  $\text{H}_2\text{S}$ , organic acids), leading to corrosion [144–146]. There is no simple mitigation method available, especially considering that the use of standard corrosion inhibitors is not feasible as they are typically liquids that do not readily evaporate and cannot reach the affected portions of the pipeline. This type of attack is very dependent on the rate of water condensation, temperature, and solubility of corrosion products. A key aspect of understanding the mechanism is the interaction between water condensation, corrosion, evolution of the chemistry in the condensed water, and formation of the corrosion product layers (usually iron carbonate) [147,148].

## 7.7 Effect of crude oil

In some cases the crude oil contains compounds that adsorb onto the steel surface either during oil wetting periods or by first partitioning into the water phase [139,149,150]. The most common surface active organic compounds found in crude

oil that have surfactant properties are those containing oxygen, sulfur, and nitrogen in their molecular structure. Furthermore, both asphaltenes and waxes have shown some beneficial inhibitive effects on corrosion [151]. Our present understanding of these phenomena is at best qualitative, making it virtually impossible to make any reliable predictions. When it comes to the effects of wetting, as described earlier, various crude oils have widely varying capacities to entrain water. Typically it takes much higher flow rates for light oils to entrain water ( $v > 1.5$  m/s) because of their lower density and viscosity. Some heavier oils are able to do the same at velocities as low as 0.5 m/s. However, the chemical composition of crude oils, particularly the content of surface active substances, is just as important for wettability as are their physical properties.

## 7.8 Localized corrosion

There are many causes of localized CO<sub>2</sub> corrosion. In general, localized corrosion will occur at locations where important factors affecting corrosion (listed later in the discussion) are significantly different from elsewhere on the surface of the same structure. Such locations may therefore become local anodes with a higher local rate of iron dissolution, with respect to the rest of the structure surface. Localization of corrosion covers a broad range of length scales. In some cases, localized corrosion amounts to having a section of a pipeline measured in meters corroding much faster than the rest of the pipeline measured in kilometers (see Fig. 7.11(a)). This could happen, for example, as a result of water accumulation at a low spot in a line. On the other end of the spectrum, we can have very small pits, measured in millimeters, propagating much faster than the large surface area around it, measured in meters, that remains unaffected by corrosion. An example would be microbiological attack shown in Fig. 7.11(b), or one could have a pit micrometers in size, with millimeters of the metal surface around it not corroding at all (see Fig. 7.11(c)).

Factors that can lead to localized corrosion of mild steel in CO<sub>2</sub> solutions may be flow related, chemical, metallurgical, or biological. Each of these four main categories can be further refined, as follows:

- Flow-related causes of localized CO<sub>2</sub> corrosion
  - Mechanical (momentum transfer related)
    - Water settling and water wetting
    - Solids settling and under-deposit attack
    - Droplet impingement
    - Solids impingement and erosion
  - Thermal (heat transfer related)
    - Water condensation in wet gas flow
    - Cavitation
  - Mixing (mass transfer related)
    - Transport of corrosive species to the metal surface
    - Transport of corrosion products away from metal surface

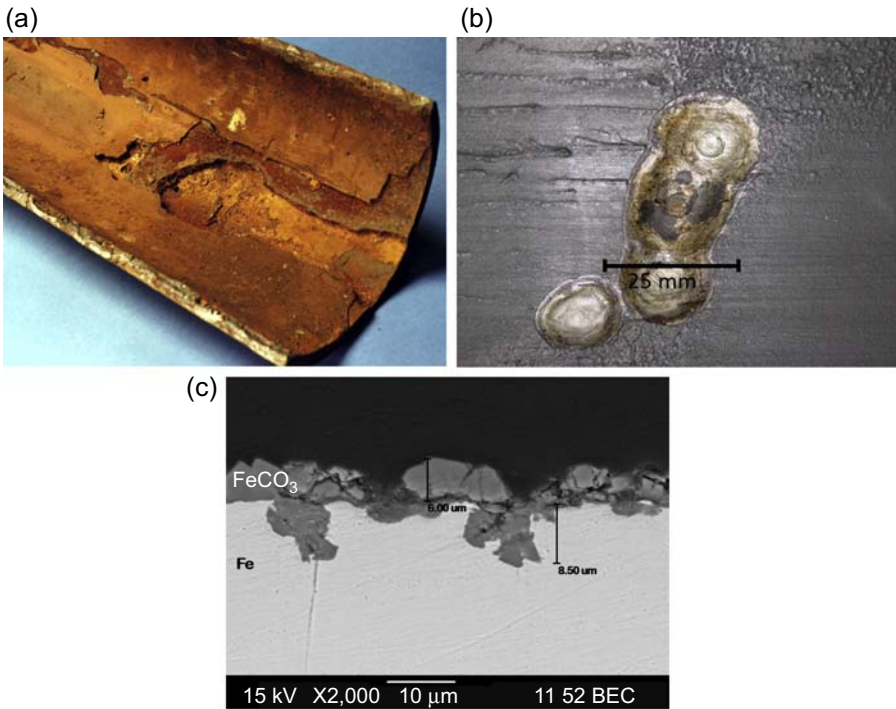


**Figure 7.11** Localized corrosion at different scales. (a) Section of a pipeline exhibiting severe localized corrosion due to solids and bacteria growth at the groove. (b) Top surface of a pipeline section exhibiting a pit due to microbially induced corrosion attack. (c) A cross-section of mild steel surface showing failure of an iron carbonate protective corrosion product layer and localized attack due to the presence of acetic acid.

- Chemical-related causes of localized  $\text{CO}_2$  corrosion
  - Poor or partial inhibition
  - Change of pH
  - High chlorides and/or ionic strength
  - Organic acids
  - Oxygen
  - $\text{H}_2\text{S}$  and elemental sulfur
- Metallurgical
  - Inclusions
  - Welds
  - Iron carbide
- Biological
  - Sulfur-reducing bacteria
  - Acid-producing bacteria

In many cases, the various effects are intertwined and cannot be readily separated. For example, flow may affect the rate of chemical processes via mass transfer, leading to a rapid dissolution of a protective corrosion product layer, or a chemical change can

be at the root of biologically induced localized corrosion by acid-producing bacteria, and so on. Clearly, there are many factors whose variation across the metal surface may lead to localized corrosion, including some that may not be covered by the aforementioned list. A comprehensive explanation of all these exceeds the scope of the present review. However, in most cases the final effect amounts to local failure of a protective layer, whether a corrosion product layer or an inhibitor film. In some situations, this is aggravated by a galvanic effect that may result in localized corrosion rates exceeding the bare steel corrosion rate [152].

## 7.9 Inhibition of CO<sub>2</sub> corrosion

Mild steel corrosion can be significantly reduced by the addition of corrosion inhibitors. These inhibitors are defined as chemicals that retard corrosion when added to an environment in small concentrations [153]. Typical organic corrosion inhibitors are cationic surfactant compounds with an amphiphilic molecular structure. They are often referred to as film forming as they form very thin protective films by adsorbing at steel surfaces [154–156]. The amphiphilic inhibitor molecules consist of a polar head group and a nonpolar hydrocarbon tail. Polar head groups are often based on nitrogen-containing groups, such as amines, amides, quaternary ammonium, or imidazoline-based salts, as well as functional groups containing oxygen, phosphorus, and/or sulfur atoms. The length of a hydrocarbon tail, which is attached to a polar group, varies between 12 and 18 carbon atoms [155]. Fig. 7.12 shows some common corrosion inhibitor molecules, with thioglycolic acid included, as it is commonly added to inhibitor “packages” (complex formulations containing a wide range of compounds used in field applications).

Corrosion inhibitor molecules, being surfactant compounds, form molecular aggregates in a bulk solution when they exceed the solubility limit. The concentration at which the molecules begin to aggregate is termed the *critical micelle concentration* (CMC) [157,158]. At or above the CMC, the inhibitor molecules will form ordered molecular structures as well as adsorbed surfactant monolayers or bilayers on metal surfaces. At hydrophilic surfaces, more than one layer of surfactant molecules can form. As a result, corrosion inhibitors are more effective at concentrations above CMC than soluble inhibitor systems below the CMC [159].

The function of the polar head groups is to provide bonding between inhibitor molecules and the steel surface. This can be achieved by chemisorption, whereby polar

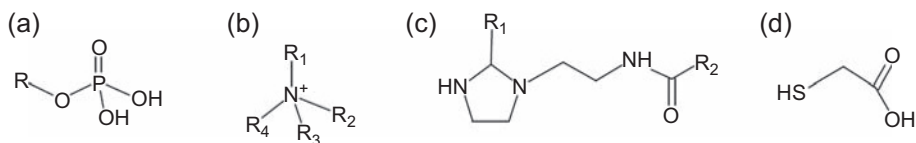


**Figure 7.12** Examples of common organic corrosion inhibitors: (a) phosphate esters, (b) quaternary ammonium salts, (c) amidoethylimidazolines, and (d) thioglycolic acid.

Reprint with permission from Marian Babic, Role of Interfacial Chemistry on Wettability and Carbon Dioxide Corrosion of Mild Steels (Doctoral dissertation), Ohio University, 2017.

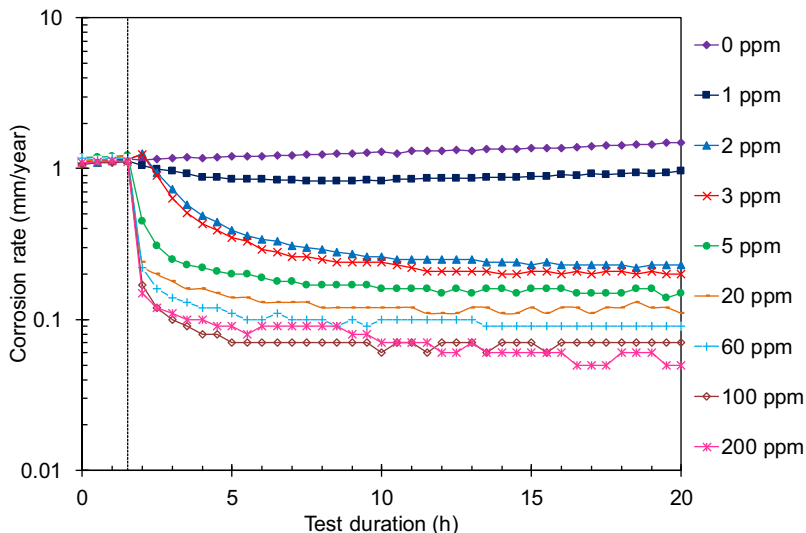


**Figure 7.13** Corrosion rates obtained by linear polarization resistance measurements for different concentrations of fatty amine corrosion inhibitor. The *vertical dotted line* indicates when the inhibitor was introduced to the solution.

Data taken from C. Li, S. Richter, S. Nešić, How do inhibitors mitigate corrosion in oil-water two-phase flow beyond lowering the corrosion rate? *Corrosion* 70 (2014) 958–967.

groups develop intramolecular bonds at and with the surface, or by physisorption whereby they are bound to the surface by intermolecular forces [156]. Hydrophobic tails, which are facing the aqueous phase, provide a diffusion barrier for corrosive species because of steric repulsion of the hydrophobic tails [160]. Fig. 7.13 shows the measured corrosion rate as a function of inhibitor concentrations for one fatty amino surfactant-based corrosion inhibitor [161]. As can be seen from Fig. 7.13, the inhibition efficiency enhances with an increase of the inhibitor concentration.

The use of corrosion inhibitors is often considered as the most cost-effective solution for corrosion control in wells, pipelines, and production facilities carrying sweet or mildly sour wet hydrocarbons. The integrity of such structures heavily relies on the effectiveness of the corrosion inhibition program in place. Corrosion inhibition is not selected in the same way for different methods of production. Similarly, good corrosion control will vary with different fluid compositions, environmental conditions, production rates, and different flow regimes.

Gregg and Ramachandran highlighted the many different approaches for developing the proper chemistry of inhibitors for subsea applications [162]. Likewise, Cassidy provided ideas for design of inhibitors for acid corrosion mitigation [163]. One of the focus areas in corrosion inhibitor development technology is in providing environmentally safe chemicals that perform well at elevated temperatures. Inhibitor partitioning between the aqueous and hydrocarbon phases and compatibility with the other injected chemicals are additional issues that need to be considered. Interaction of inhibitors with corrosion product layers and scales, particularly various forms of iron sulfide, remains a poorly understood phenomenon.

## 7.10 Some field experiences and key challenges

Generally, the failure to control CO<sub>2</sub> corrosion in the field is often not due to the lack of understanding of corrosion, it is rather due to a failure to predict its extent and to design and implement the appropriate mitigation program. Depending on the CO<sub>2</sub> content, temperature, and pH, using corrosion-resistant alloys to control CO<sub>2</sub> corrosion is first assessed with respect to cost-effectiveness. If the cost is prohibitive, the option of using mild steel and inhibition is typically adopted. The following are some pointers indicating various types of field assets exposed to corrosion, the range of operating parameters where corrosion issues are found, and challenges to control CO<sub>2</sub> corrosion in the field.

Assets subject to CO<sub>2</sub> corrosion:

- Downhole tubing strings in gas and oil wells (e.g., rod pump wells, electrical submersible pump wells, gas lift wells)
- Casing strings exposed to production by design or due to communication through the annulus
- Wellhead equipment
- Flow lines
- Facilities (e.g., compressors, pumps, tanks, separators, valves)
- Transfer lines and piping
- Wet gas pipelines
- Oil export pipelines

Typical operating parameters:

- CO<sub>2</sub> content: 0.2–40 mol% in the gas phase
- Temperature: 16°C (60°F)–163°C (325°F)
- pH range: 3.5–6.5
- Flow regimes: slug, annular mist, stratified
- Flow rates: liquid velocities: 0.5–5 m/s, gas velocities: 5–20 m/s

Some of the key challenges are grouped in the following as *mechanism and prediction*, *inhibition*, and *monitoring/inspection*.

- Mechanism and prediction:
  - There is a lack of prediction models for CO<sub>2</sub> pitting corrosion; laboratory testing is not always possible and might not properly simulate the actual field conditions.
  - Prediction of CO<sub>2</sub> corrosion with traces of H<sub>2</sub>S present in the production system is unreliable.
  - Synergy between CO<sub>2</sub> corrosion and erosion in rod pump wells.
  - Integrity of iron carbonate corrosion product layers and their effect on the corrosion rate.
- Inhibition:
  - Inhibitor effectiveness in high-temperature high-pressure environments: lack of clear limits of temperature and CO<sub>2</sub> content for effective inhibition.
  - Inhibitor ability to suppress pitting, to control preferential weld corrosion, and to perform in the presence of solids.
  - Inhibitor partitioning into the water phase.
  - Inhibitor transport in pipelines, in particular in wet gas pipelines, to manage TLC.
  - Application of corrosion inhibitors for downhole treatments.

- Prediction of corrosion inhibitor persistency for batch applications.
- Environment friendly “green” chemistries with acceptable effectiveness and cost.
- Monitoring/inspection:
  - Interpretation of caliper survey pitting data for wells.
  - Interpretation of ILI (in Line Inspection) magnetic flux leakage and ultrasonic testing survey data for pipelines.
  - Monitoring of corrosion inhibitor residuals.
  - Prediction of critical corrosion locations for monitoring program design.

## References

- [1] W. Stumm, J.J. Morgan, *Aquatic Chemistry: Chemical Equilibria and Rates in Natural Waters*, 1995.
- [2] R.E. Zeebe, D. Wolf-Gladrow (Eds.), *CO<sub>2</sub> in Seawater: Equilibrium, Kinetics, Isotopes*, Elsevier, 2001.
- [3] J.N. Butler, *Carbon Dioxide Equilibria and Their Applications*, CRC Press, 1991.
- [4] Z. Duan, R. Sun, An improved model calculating CO<sub>2</sub> solubility in pure water and aqueous NaCl solutions from 273 to 533 K and from 0 to 2000 bar, *Chemical Geology* 193 (2003) 257–271.
- [5] Z. Duan, D. Li, Coupled phase and aqueous species equilibrium of the H<sub>2</sub>O–CO<sub>2</sub>–NaCl–CaCO<sub>3</sub> system from 0 to 250°C, 1 to 1000 bar with NaCl concentrations up to saturation of halite, *Geochimica et Cosmochimica Acta* 72 (2008) 5128–5145.
- [6] Z. Duan, R. Sun, C. Zhu, I.-M. Chou, An improved model for the calculation of CO<sub>2</sub> solubility in aqueous solutions containing Na<sup>+</sup>, K<sup>+</sup>, Ca<sup>2+</sup>, Mg<sup>2+</sup>, Cl<sup>-</sup>, and SO<sub>4</sub><sup>2-</sup>, *Marine Chemistry* 98 (2006) 131–139.
- [7] D. Li, Z. Duan, The speciation equilibrium coupling with phase equilibrium in the H<sub>2</sub>O–CO<sub>2</sub>–NaCl system from 0 to 250°C, from 0 to 1000 bar, and from 0 to 5 molality of NaCl, *Chemical Geology* 244 (2007) 730–751.
- [8] D.A. Palmer, R. Van Eldik, The chemistry of metal carbonate and carbon dioxide complexes, *Chemical Reviews* 83 (1983) 651–731.
- [9] R.F. Weiss, Carbon dioxide in water and sea water: the solubility of a non-ideal gas, *Marine Chemistry* 2 (1974) 203–215.
- [10] T. Barth, Organic acids and inorganic ions in waters from petroleum reservoirs, Norwegian continental shelf: a multivariate statistical analysis and comparison with American reservoir formation waters, *Applied Geochemistry* 6 (1991) 1–15.
- [11] T.I.R. Utvik, Chemical characterization of produced water from four offshore oil production platforms in the North Sea, *Chemosphere* 39 (1999) 2593–2606.
- [12] J. Han, J. Zhang, J.W. Carey, Effect of bicarbonate on corrosion of carbon steel in CO<sub>2</sub> saturated brines, *International Journal of Greenhouse Gas Control* 5 (2011) 1680–1683.
- [13] G.I. Ogundele, W.E. White, Some observations on corrosion of carbon steel in aqueous environments containing carbon dioxide, *Corrosion* 42 (1986) 71–78.
- [14] G.I. Ogundele, W.E. White, Observations on the influences of dissolved hydrocarbon gases and variable water chemistries on corrosion of an API-L80 steel, *Corrosion* 43 (1987) 665–673.
- [15] L.G.S. Gray, B.G. Anderson, M.J. Danysh, P.R. Tremaine, Effect of pH and temperature on the mechanism of carbon steel corrosion by aqueous carbon dioxide, in: *CORROSION* 90, Paper No. 40.

- [16] J.O. Bockris, D. Drazic, The kinetics of deposition and dissolution of iron: effect of alloying impurities, *Electrochimica Acta* 7 (1962) 293–313.
- [17] F. Hibert, Y. Miyoshi, G. Eichkorn, W.J. Lorenz, Correlations between the kinetics of electrolytic dissolution and deposition of iron, *Journal of the Electrochemical Society* 118 (1971) 1919–1926.
- [18] A. Atkinson, A. Marshall, Anodic dissolution of iron in acidic chloride solutions, *Corrosion Science* 18 (1978) 427–439.
- [19] A.A. El Miligy, D. Geana, W.J. Lorenz, A theoretical treatment of the kinetics of iron dissolution and passivation, *Electrochimica Acta* 20 (1975) 273–281.
- [20] S. Nešić, N. Thevenot, J.L. Crolet, D. Drazic, Electrochemical properties of iron dissolution in the presence of CO<sub>2</sub>-basics revisited, in: *CORROSION 1996*, Paper No. 03.
- [21] M. Keddam, O.R. Mattos, H. Takenout, Reaction model for iron dissolution studied by electrode impedance. I. Experimental results and reaction model, *Journal of the Electrochemical Society* 128 (1981) 257–266.
- [22] M. Keddam, O.R. Mattos, H. Takenout, Reaction model for iron dissolution studied by electrode impedance. II. Determination of the reaction model, *Journal of the Electrochemical Society* 128 (1981) 266–274.
- [23] L. Felloni, The effect of pH on the electrochemical behaviour of iron in hydrochloric acid, *Corrosion Science* 8 (1968) 133–148.
- [24] J.O. Bockris, D. Drazic, A.R. Despic, The electrode kinetics of the deposition and dissolution of iron, *Electrochimica Acta* 4 (1961) 325–361.
- [25] D. Drazic, Iron and its electrochemistry in an active state, *Modern Aspects of Electrochemistry* 19 (1989) 62–192.
- [26] D.M. Dražić, C.S. Hao, The anodic dissolution process on active iron in alkaline solutions, *Electrochimica Acta* 27 (1982) 1409–1415.
- [27] W.J. Lorenz, G. Staikov, W. Schindler, W. Wiesbeck, The role of low-dimensional systems in electrochemical phase formation and dissolution processes, *Journal of the Electrochemical Society* 149 (2002) K47–K59.
- [28] M. Keddam, Anodic dissolution, in: *Corros. Mech. Theory Pract*, third ed., CRC Press, 2011, pp. 149–215.
- [29] S. Nešić, J. Postlethwaite, S. Olsen, An electrochemical model for prediction of corrosion of mild steel in aqueous carbon dioxide solutions, *Corrosion* 52 (1996) 280–294.
- [30] L.G.S. Gray, B.G. Anderson, M.J. Danysh, P.R. Tremaine, Mechanisms of carbon steel corrosion in brines containing dissolved carbon dioxide at pH 4, in: *CORROSION 1989*, Paper No. 464.
- [31] K.E. Heusler, *Encyclopedia of Electrochemistry of the Elements*, vol. 9, Marcel Dekker, New York, 1982.
- [32] K.S. George, S. Nešić, Investigation of carbon dioxide corrosion of mild steel in the presence of acetic acid-part I: basic mechanisms, *Corrosion* (2007) 178–186.
- [33] F.M. Song, A comprehensive model for predicting CO<sub>2</sub> corrosion rate in oil and gas production and transportation systems, *Electrochimica Acta* 55 (2010) 689–700.
- [34] F.M. Song, D.W. Kirk, J.W. Graydon, D.E. Cormack, CO<sub>2</sub> corrosion of bare steel under an aqueous boundary layer with oxygen, *Journal of the Electrochemical Society* 149 (2002) B479–B486.
- [35] A. Anderko, R.D. Young, Simulation of CO<sub>2</sub>/H<sub>2</sub>S corrosion using thermodynamic and electrochemical models, in: *CORROSION 1999*, Paper No. 31.
- [36] J. Han, J.W. Carey, J. Zhang, A coupled electrochemical-geochemical model of corrosion for mild steel in high-pressure CO<sub>2</sub>-saline environments, *International Journal of Greenhouse Gas Control* 5 (2011) 777–787.

- [37] J.K. Nørskov, T. Bligaard, a. Logadottir, J.R. Kitchin, J.G. Chen, S. Pandelov, et al., Trends in the exchange current for hydrogen evolution, *Journal of the Electrochemical Society* 152 (2005) J23.
- [38] J.O. Bockris, D.F.A. Koch, Comparative rates of the electrolytic evolution of hydrogen and deuterium on iron, tungsten and platinum, *The Journal of Physical Chemistry* 65 (1961) 1941–1948.
- [39] Y. Xu, The hydrogen evolution reaction on single crystal gold electrode, *International Journal of Hydrogen Energy* 34 (2009) 77–83.
- [40] M.A.V. Devanathan, Z. Stachurski, The mechanism of hydrogen evolution on iron in acid solutions by determination of permeation rates, *Journal of the Electrochemical Society* 111 (1964) 619–623.
- [41] J.O. Bockris, E.C. Potter, The mechanism of the cathodic hydrogen evolution reaction, *Journal of the Electrochemical Society* 99 (1952) 169.
- [42] N. Pentland, J.O. Bockris, E. Sheldon, Hydrogen evolution reaction on copper, gold, molybdenum, palladium, rhodium, and iron, *Journal of the Electrochemical Society* 104 (1957) 182.
- [43] J.O. Bockris, J. McBreen, L. Nanis, The hydrogen evolution kinetics and hydrogen entry into  $\alpha$ -iron, *Journal of the Electrochemical Society* 112 (1965) 1025–1031.
- [44] A. Lasia, A. Rami, Kinetics of hydrogen evolution on nickel electrodes, *Journal of Electroanalytical Chemistry and Interfacial Electrochemistry* 294 (1990) 123–141.
- [45] B.E. Conway, B.V. Tilak, Interfacial processes involving electrocatalytic evolution and oxidation of  $H_2$ , and the role of chemisorbed H, *Electrochimica Acta* 47 (2002) 3571–3594.
- [46] K. Juodkazis, J. Juodkazyte, B. Šebeka, S. Juodkazis, Reversible hydrogen evolution and oxidation on Pt electrode mediated by molecular ion, *Applied Surface Science* 290 (2014) 13–17.
- [47] K. Juodkazis, J. Juodkazyt, A. Grigučevičien, S. Juodkazis, Hydrogen species within the metals: role of molecular hydrogen ion  $H_2^+$ , *Applied Surface Science* 258 (2011) 743–747.
- [48] N.T. Thomas, K. Nobe, Kinetics of the hydrogen evolution reaction on titanium, *Journal of the Electrochemical Society* 117 (1970) 622.
- [49] S. Schuldiner, Kinetics of hydrogen evolution at zero hydrogen partial pressure, *Journal of the Electrochemical Society* 108 (1961) 384.
- [50] J.O. Bockris, I.A. Ammar, A.K.M.S. Huq, The mechanism of the hydrogen evolution reaction on platinum silver and tungsten surfaces in acid solutions, *The Journal of Physical Chemistry* 61 (1957) 879–886.
- [51] G.J. Brug, M. Sluyters-Rehbach, J.H. Sluyters, A. Hemelin, The kinetics of the reduction of protons at polycrystalline and monocrystalline gold electrodes, *Journal of Electroanalytical Chemistry* 181 (1984) 245–266.
- [52] W. Sheng, H.A. Gasteiger, Y. Shao-Horn, Hydrogen oxidation and evolution reaction kinetics on platinum: acid vs alkaline electrolytes, *Journal of the Electrochemical Society* 157 (2010) B1529–B1536.
- [53] S. Schuldiner, Hydrogen overvoltage on bright platinum II. pH and salt effects in acid, neutral, and alkaline solutions, *Journal of the Electrochemical Society* 101 (1954) 426–432.
- [54] S.Y. Qian, B.E. Conway, G. Jerkiewicz, Kinetic rationalization of catalyst poison effects on cathodic H sorption into metals: relation of enhancement and inhibition to H coverage, *Journal of the Chemical Society, Faraday Transactions* 94 (1998) 2945–2954.

- [55] S.Y. Qian, B.E. Conway, G. Jerkiewicz, Electrochemical sorption of H into Fe and mild-steel: kinetic conditions for enhancement or inhibition by adsorbed HS<sup>-</sup>, *Physical Chemistry Chemical Physics* 1 (1999) 2805–2813.
- [56] Y. Zheng, B. Brown, S. Nešić, Electrochemical study and modeling of H<sub>2</sub>S corrosion of mild steel, *Corrosion* 70 (2014) 351–365.
- [57] T. Tran, B. Brown, S. Nešić, Investigation of the electrochemical mechanisms for acetic acid corrosion of mild steel, *Corrosion* 70 (2014) 223–229.
- [58] E. Remita, B. Tribollet, E. Sutter, V. Vivier, F. Ropital, J. Kittel, Hydrogen evolution in aqueous solutions containing dissolved CO<sub>2</sub>: quantitative contribution of the buffering effect, *Corrosion Science* 50 (2008) 1433–1440.
- [59] B. Tribollet, J. Kittel, A. Meroufel, F. Ropital, F. Grosjean, E.M.M. Sutter, Corrosion mechanisms in aqueous solutions containing dissolved H<sub>2</sub>S. Part 2: model of the cathodic reactions on a 316L stainless steel rotating disc electrode, *Electrochimica Acta* 124 (2014) 46–51.
- [60] J. Kittel, F. Ropital, F. Grosjean, E.M.M. Sutter, B. Tribollet, Corrosion mechanisms in aqueous solutions containing dissolved H<sub>2</sub>S. Part 1: characterisation of H<sub>2</sub>S reduction on a 316L rotating disc electrode, *Corrosion Science* 66 (2013) 324–329.
- [61] P. Delahay (Ed.), *Advances in Electrochemistry and Electrochemical Engineering: Volume 7 Electrochemistry*, Interscience, 1970.
- [62] B.E. Conway, M. Salomon, Electrochemical reaction orders: applications to the hydrogen- and oxygen-evolution reactions, *Electrochimica Acta* 9 (1964) 1599–1615.
- [63] R.J. Chin, K. Nobe, Electrodeposition kinetics of iron in chloride solutions III. Acidic solutions, *Journal of the Electrochemical Society* 119 (1972) 1457–1461.
- [64] T. Hurlen, Electrochemical behaviour of iron, *Acta Chemica Scandinavica* 14 (1960) 1533–1554.
- [65] E. McCafferty, N. Hackerman, Kinetics of iron corrosion in concentrated acid chloride solutions, *Journal of the Electrochemical Society* 119 (1972) 999–1009.
- [66] M. Stern, The electrochemical behavior, including hydrogen overvoltage, of iron in acid environments, *Journal of the Electrochemical Society* 102 (1955) 609–616.
- [67] J. Amri, E. Gulbrandsen, R.P. Nogueira, Role of acetic acid in CO<sub>2</sub> top of the line corrosion of carbon steel, in: *CORROSION 2011*, Paper No. 329.
- [68] A. Więckowski, E. Ghali, M. Szklarczyk, J. Sobkowski, The behaviour of iron electrode in CO<sub>2</sub><sup>-</sup> saturated neutral electrolyte—II. Radiotracer study and corrosion considerations, *Electrochimica Acta* 28 (1983) 1627–1633.
- [69] B. Mishra, S. Al-Hassan, D.L. Olson, M.M. Salama, Development of a predictive model for activation-controlled corrosion of steel in solutions containing carbon dioxide, *Corrosion* 53 (1997) 852–859.
- [70] A. Więckowski, E. Ghali, M. Szklarczyk, J. Sobkowski, The behaviour of iron electrode in CO<sub>2</sub><sup>-</sup> saturated neutral electrolyte—I. Electrochemical study, *Electrochimica Acta* 28 (1983) 1619–1626.
- [71] M. Nordsveen, S. Nešić, R. Nyborg, A. Stangeland, A mechanistic model for carbon dioxide corrosion of mild steel in the presence of protective iron carbonate films – part 1: theory and verification, *Corrosion* 59 (2003) 443–456.
- [72] S. Nešić, M. Nordsveen, R. Nyborg, A. Stangeland, A mechanistic model for CO<sub>2</sub> corrosion with protective iron carbonate films, in: *CORROSION 2001*, Paper No. 040.
- [73] A. Kahyarian, M. Singer, S. Nestic, Modeling of uniform CO<sub>2</sub> corrosion of mild steel in gas transportation systems: a review, *Journal of Natural Gas Science and Engineering* 29 (2016) 530–549.

- [74] Y. Zheng, J. Ning, B. Brown, S. Nescic, Electrochemical model of mild steel corrosion in a mixed H<sub>2</sub>S/CO<sub>2</sub> aqueous environment, *Corrosion* 2014 (71) (2014) 316.
- [75] W.M. Haynes, *CRC Handbook of Chemistry and Physics*, 2009.
- [76] B.R. Linter, G.T. Burstein, Reactions of pipeline steels in carbon dioxide solutions, *Corrosion Science* 41 (1999) 117–139.
- [77] C. De Waard, D.E. Milliams, Carbonic acid corrosion of steel, *Corrosion* 31 (1975) 177–181.
- [78] G. Schmitt, B. Rothmann, Studies on the corrosion mechanism of unalloyed steel in oxygen-free carbon dioxide solutions part I. Kinetics of the liberation of hydrogen, *Werkstoffe Und Korrosion* 28 (1977) 816.
- [79] B.F.M. Pots, Mechanistic models for the prediction of CO<sub>2</sub> corrosion rates under multiphase flow conditions, in: *CORROSION 1995*, Paper No. 137.
- [80] S. Turgoose, R.A. Cottis, K. Lawson, Modeling of electrode processes and surface chemistry in carbon dioxide containing solutions, in: *Comput. Model. Corros. ASTM STP 1154*, 1992, pp. 67–81.
- [81] C. de Waard, D.E. Milliams, Prediction of carbonic acid corrosion in natural gas pipelines, in: *Intern. Extern. Prot. Pipes*, 1975. F1-1–F1-8.
- [82] S. Nešić, J. Lee, V. Ruzic, A mechanistic model of iron carbonate film growth and the effect on CO<sub>2</sub> corrosion of mild steel, in: *CORROSION 2002*, Paper No. 237.
- [83] S. Nešić, M. Nordsveen, R. Nyborg, A. Stangeland, A mechanistic model for carbon dioxide corrosion of mild steel in the presence of protective iron carbonate films—Part 2: a numerical experiment, *Corrosion* 59 (2003) 489–497.
- [84] S. Nešić, K. Lee, A mechanistic model for carbon dioxide corrosion of mild steel in the presence of protective iron carbonate films - Part 3: film growth model, *Corrosion* (2003) 616–628.
- [85] T.J. Gray, R.B. Rozelle, M.L. Soeder, Catalytic investigations using galvanostatic techniques, *Nature* 202 (1964) 181–182.
- [86] A. Kahyarian, B. Brown, S. Nescic, Mechanism of cathodic reactions in acetic acid corrosion of iron and mild steel, *Corrosion* 72 (2016) 1539–1546.
- [87] S.N. Esmaeely, B. Brown, S. Nescic, Verification of an electrochemical model for aqueous corrosion of mild steel for H<sub>2</sub>S partial pressures up to 0.1 Mpa, *Corrosion* 73 (2017) 144–154.
- [88] T. Tran, B. Brown, S. Nešić, Corrosion of mild steel in an aqueous CO<sub>2</sub> environment – basic electrochemical mechanisms revisited, in: *CORROSION 2015*, Paper No. 671.
- [89] C. de Waard, U. Lotz, A. Dugstad, Influence of liquid flow velocity on CO<sub>2</sub> corrosion: a semi-empirical model, in: *CORROSION 95*, Paper No. 128.
- [90] U. Lotz, Velocity effects in flow induced corrosion, in: *CORROSION 1990*, Paper No. 27.
- [91] A. Dugstad, L. Lunde, K. Videm, Parametric study of CO<sub>2</sub> corrosion of carbon steel, in: *CORROSION 1994*, Paper No. 14.
- [92] S. Nescic, G.T. Solvi, J. Enerhaug, Comparison of the rotating cylinder and pipe flow tests for flow-sensitive carbon dioxide corrosion, *Corrosion* 51 (1995) 773–787.
- [93] A. Mohammed Nor, M.F. Suhor, M.F. Mohamed, M. Singer, S. Nešić, Corrosion of carbon steel in high CO<sub>2</sub> environment: flow effect, in: *CORROSION 2011*, Paper No. 242.
- [94] M. Eisenberg, C.W. Tobias, C.R. Wilke, Ionic mass transfer and concentration polarization at rotating electrodes, *Journal of the Electrochemical Society* 101 (1954) 306–320.
- [95] D.C. Silverman, Practical corrosion prediction using electrochemical techniques, in: *Uhlig's Corros. Handb.*, John Wiley & Sons, Inc., 2011, pp. 1129–1166.

- [96] F.P. Berger, K.-F.F.-L. Hau, Mass transfer in turbulent pipe flow measured by the electrochemical method, *International Journal of Heat and Mass Transfer* 20 (1977) 1185–1194.
- [97] M.W.E. Coney, *Erosion-Corrosion: The Calculation of Mass-Transfer Coefficients*, 1981.
- [98] B. Poulson, Measuring and modelling mass transfer at bends in annular two phase flow, *Chemical Engineering Science* 46 (1991) 1069–1082.
- [99] J. Wang, S.A. Shirazi, J.R. Shadley, E.F. Rybicki, E. Dayalan, A correlation for mass transfer coefficients in elbows, in: *CORROSION 1998*, Paper No. 42.
- [100] J. Wang, S.A. Shirazi, A CFD based correlation for mass transfer coefficient in elbows, *International Journal of Heat and Mass Transfer* 44 (2001) 1817–1822.
- [101] E.L. Cussler, *Diffusion: Mass Transfer in Fluid Systems*, Cambridge University Press, 1997.
- [102] A.J. Bard, L.R. Faulkner, *Electrochemical Methods: Fundamentals and Applications*, John Wiley & Sons, INC., 2001.
- [103] S. Nešić, J. Postlethwaite, N. Thevenot, Superposition of diffusion and chemical reaction controlled limiting current - application to CO<sub>2</sub> corrosion, *Journal of Corrosion Science and Engineering* 1 (1995) 1–14.
- [104] S. Nešić, H. Li, J. Huang, D. Sormaz, An open source mechanistic model for CO<sub>2</sub>/H<sub>2</sub>S corrosion of carbon steel, in: *CORROSION 2009*, Paper No. 09572.
- [105] F. Farelas, B. Brown, S. Nestic, Iron carbide and its influence on the formation of protective iron carbonate in CO<sub>2</sub> corrosion of mild steel, in: *CORROSION 2013*, Paper No. 2291.
- [106] W. Sun, S. Nešić, R.C. Woollam, The effect of temperature and ionic strength on iron carbonate (FeCO<sub>3</sub>) solubility limit, *Corrosion Science* 51 (2009) 1273–1276.
- [107] S.N. Esmaeely, D. Young, B. Brown, S. Nestic, Effect of incorporation of calcium into iron carbonate protective layers in CO<sub>2</sub> corrosion of mild steel, *Corrosion* 73 (2016) 238–246.
- [108] P. Menaul, Causative agents of corrosion in distillate field, *Oil and Gas Journal* 43 (1944) 80–81.
- [109] J.L. Crolet, M.R. Bonis, The role of acetate ions in CO<sub>2</sub> corrosion, in: *CORROSION 1983*, Paper No. 160.
- [110] Y. Garsany, D. Pletcher, B. Hedges, Speciation and electrochemistry of brines containing acetate ion and carbon dioxide, *Journal of Electroanalytical Chemistry* 538–539 (2002) 285–297.
- [111] Y. Sun, K. George, S. Nestic, S. Nešić, The effect of Cl<sup>-</sup> and acetic acid on localized CO<sub>2</sub> corrosion in wet gas flow, *Corrosion* 2003 (2003) 1–28.
- [112] J.-L. Crolet, N. Thevenot, A. Dugstad, Role of free acetic acid on the CO<sub>2</sub> corrosion of steels, in: *CORROSION 1999*, Paper No. 24.
- [113] K. George, S. Nešić, C. de Waard, Electrochemical investigation and modeling of carbon dioxide corrosion of carbon steel in the presence of acetic acid, in: *CORROSION 2004*, Paper No. 379.
- [114] K. George, S. Wang, S. Nestic, C. de Waard, Modeling of CO<sub>2</sub> corrosion of mild steel at high pressures of CO<sub>2</sub> in the presence of acetic acid, in: *CORROSION 2004*, Paper No. 04623.
- [115] Y. Garsany, D. Pletcher, B. Hedges, The role of acetate in CO<sub>2</sub> corrosion of carbon steel: has the chemistry been forgotten? in: *CORROSION 2002*, Paper No. 273.
- [116] B. Hedges, L. Mcveigh, The role of acetate in CO<sub>2</sub> corrosion: the double whammy, in: *CORROSION 1999*, Paper No. 21.

- [117] M.W. Joosten, J. Kolts, J.W. Hembree, P. City, M. Achour, Organic acid corrosion in oil and gas production, in: CORROSION 2002, Paper No. 294.
- [118] V. Fajardo, C. Canto, B. Brown, S. Nešić, Effects of organic acids in CO<sub>2</sub> corrosion, in: CORROSION 2007, Paper No. 319.
- [119] E. Gulbrandsen, K. Bilkova, Solution chemistry effects on corrosion of carbon steels in presence of CO<sub>2</sub> and acetic acid, in: CORROSION 2006, Paper No. 364.
- [120] M. Matos, C. Canhoto, M.F. Bento, M.D. Geraldo, Simultaneous evaluation of the dissociated and undissociated acid concentrations by square wave voltammetry using microelectrodes, *Journal of Electroanalytical Chemistry* 647 (2010) 144–149.
- [121] P.C. Okafor, B. Brown, S. Nešić, CO<sub>2</sub> corrosion of carbon steel in the presence of acetic acid at higher temperatures, *Journal of Applied Electrochemistry* 39 (2009) 873–877.
- [122] J. Amri, E. Gulbrandsen, R.P. Nogueira, Pit growth and stifling on carbon steel in CO<sub>2</sub>-containing media in the presence of HAc, *Electrochimica Acta* 54 (2009) 7338–7344.
- [123] T. Hurlen, S. Gunvaldsen, F. Blaker, Effects of buffers on hydrogen evolution at iron electrodes, *Electrochimica Acta* 29 (1984) 1163–1164.
- [124] K.S. George, *Electrochemical Investigation of Carbon Dioxide Corrosion of Mild Steel in the Presence of Acetic Acid* (Doctoral dissertation), Ohio University, 2003.
- [125] J. Amri, E. Gulbrandsen, R.P. Nogueira, Propagation and arrest of localized attacks in carbon dioxide corrosion of carbon steel in the presence of acetic acid, *Corrosion* 66 (2010) 035001/1–035001/7.
- [126] J. Amri, E. Gulbrandsen, R.P. Nogueira, Numerical simulation of a single corrosion pit in CO<sub>2</sub> and acetic acid environments, *Corrosion Science* 52 (2010) 1728–1737.
- [127] J. Amri, E. Gulbrandsen, R.P. Nogueira, The effect of acetic acid on the pit propagation in CO<sub>2</sub> corrosion of carbon steel, *Electrochemistry Communications* 10 (2008) 200–203.
- [128] H. Fang, B. Brown, S. Nestic, High salt concentration effects on CO<sub>2</sub> corrosion and H<sub>2</sub>S corrosion, in: CORROSION 2010, Paper No. 10276.
- [129] H. Fang, *Low Temperature and High Salt Concentration Effects on General CO<sub>2</sub> Corrosion for Carbon Steel* (M.S. thesis), Ohio University, 2006.
- [130] G.B. Wallis, *One-Dimensional Two-Phase Flow*, McGraw-Hill, New York, 1969.
- [131] O. Shoham, *Mechanistic Modeling of Gas-Liquid Two-Phase Flow in Pipes*, Society of Petroleum Engineers, Richardson, TX, 2006.
- [132] Y. Taitel, N. Lee, A.E. Dukler, Transient gas-liquid flow in horizontal pipes: modeling the flow pattern transitions, *AIChE Journal* 24 (1978) 920–934.
- [133] W. Li, B.F.M. Pots, B. Brown, K.E. Kee, S. Nestic, A direct measurement of wall shear stress in multiphase flow – is it an important parameter in CO<sub>2</sub> corrosion of carbon steel pipelines? *Corrosion Science* 110 (2016) 35–45.
- [134] Y. Yang, B. Brown, S. Nestic, M.E. Gennaro, B. Molinas, Mechanical strength and removal of a protective iron carbonate layer formed on mild steel in CO<sub>2</sub> corrosion, in: CORROSION 2010, Paper No. 10383.
- [135] Y. Xiong, B. Brown, B. Kinsella, S. Nešić, A. Pailleret, Atomic force microscopy study of the adsorption of surfactant corrosion inhibitor films, *Corrosion* 70 (2014) 247–260.
- [136] Y. Yang, *Removal Mechanisms of Protective Iron Carbonate Layer in Flowing Solutions* (Doctoral dissertation), Ohio University, 2012.
- [137] W. Li, *Mechanical Effects of Flow on CO<sub>2</sub> Corrosion Inhibition of Carbon Steel Pipelines* (Doctoral dissertation), Ohio University, 2016.
- [138] K.E. Kee, S. Richter, M. Babic, S. Nešić, Experimental study of oil-water flow patterns in a large diameter flow loop-the effect on water wetting and corrosion, *Corrosion* 72 (2016) 569–582.

- [139] J. Cai, C. Li, X. Tang, F. Ayello, S. Richter, S. Nestic, Experimental study of water wetting in oil-water two phase flow-horizontal flow of model oil, *Chemical Engineering Science* 73 (2012) 334–344.
- [140] J. Addis, B. Brown, S. Nestic, Multiphase Technology, Erosion-corrosion in disturbed liquid/particle flow, in: *CORROSION 2008*, Paper No. 08572.
- [141] J.F. Addis, *Erosion-Corrosion in Disturbed Liquid/Particle Flow* (M.S. thesis), Ohio University, 2008.
- [142] J. Huang, B. Brown, X. Jiang, B. Kinsella, S. Nestic, Internal CO<sub>2</sub> corrosion of mild steel pipelines under inert solid deposits, in: *CORROSION 2010*, Paper No. 10379.
- [143] J. Huang, B. Brown, Y.-S. Choi, S. Nešić, Prediction of uniform CO<sub>2</sub> corrosion of mild steel under inert solid deposits, in: *CORROSION 2011*, Paper No. 11260.
- [144] M. Singer, D. Hinkson, Z. Zhang, H. Wang, S. Nestic, CO<sub>2</sub> top-of-the-line corrosion in presence of acetic acid: a parametric study, *Corrosion* 69 (2013) 719–735.
- [145] A.S. Ruhl, A. Kranzmann, Corrosion behavior of various steels in a continuous flow of carbon dioxide containing impurities, *International Journal of Greenhouse Gas Control* 9 (2012) 85–90.
- [146] A.S. Ruhl, A. Kranzmann, Investigation of corrosive effects of sulphur dioxide, oxygen and water vapour on pipeline steels, *International Journal of Greenhouse Gas Control* 13 (2013) 9–16.
- [147] B.F.M. Pots, E.L.J.a. Hendriksen, CO<sub>2</sub> corrosion under scaling conditions – the special case of top-of-line corrosion in wet gas pipelines, in: *CORROSION 2000*, Paper No. 031.
- [148] R. Nyborg, A. Dugstad, Top of line corrosion and water condensation rates in wet gas pipelines, in: *CORROSION 2007*, Paper No. 555.
- [149] F. Ayello, W. Robbins, S. Richter, S. Nešić, Model compound study of the mitigative effect of crude oil on pipeline corrosion, *Corrosion* 69 (2013) 286–296.
- [150] F. Ayello, *Crude Oil Chemistry Effects on Corrosion Inhibition and Phase Wetting in Oil-Water Flow* (Doctoral dissertation), Ohio University, 2010.
- [151] P. Ajmera, W. Robbins, S. Richter, S. Nestic, Role of asphaltenes in inhibiting corrosion and altering the wettability of the steel surface, *Corrosion* 67 (2011) 1–11.
- [152] J. Han, B.N. Brown, S. Nešić, Investigation of the galvanic mechanism for localized carbon dioxide corrosion propagation using the artificial pit technique, *Corrosion* 66 (2010), 950031-1–950031-12.
- [153] J.M. West, *Basic Corrosion and Oxidation*, Halsted Press, 1980.
- [154] M. Fingar, J. Jackson, Application of corrosion inhibitors for steels in acidic media for the oil and gas industry: a review, *Corrosion Science* 86 (2014) 17–41.
- [155] J.W. Palmer, W. Hedges, J.L. Dawson, *Use of Corrosion Inhibitors in Oil and Gas Production*: (EFC 39), Maney Publishing, 2004.
- [156] M.A. Kelland, *Production Chemicals for the Oil and Gas Industry*, Second edit, CRC Press, 2014.
- [157] C. Canto, *Effect of Wall Shear Stress on Corrosion Inhibitor Film* Christian Canto (Doctoral dissertation), Ohio University, 2010.
- [158] L.G. Qiu, A.J. Xie, Y.H. Shen, The adsorption and corrosion inhibition of some cationic gemini surfactants on carbon steel surface in hydrochloric acid, *Corrosion Science* 47 (2005) 273–278.
- [159] V. Jovancicevic, S. Ramachandran, P. Prince, Inhibition of CO<sub>2</sub> corrosion of mild steel by imidazolines and their precursors, *Corrosion* 55 (1999) 449–455.

- [160] M.E. Palomar, C.O. Olivares-Xometl, N.V. Likhanova, J.B. Pérez-Navarrete, Imidazolium, pyridinium and dimethyl-ethylbenzyl ammonium derived compounds as mixed corrosion inhibitors in acidic medium, *Journal of Surfactants and Detergents* 14 (2011) 211–220.
- [161] C. Li, S. Richter, S. Nešić, How do inhibitors mitigate corrosion in oil-water two-phase flow beyond lowering the corrosion rate? *Corrosion* 70 (2014) 958–967.
- [162] M.R. Gregg, S. Ramachandran, Review of corrosion inhibitor developments and testing for offshore oil and gas production systems, in: *CORROSION 2004*, Paper No. 04422.
- [163] J.M. Cassidy, Design and investigation of a north sea acid corrosion inhibition system, in: *CORROSION 2006*, Paper No. 482.